Physiol Rev
82: 735–767, 2002; 10.1152/physrev.00007.2002.

Epithelial Sodium Channel/Degenerin Family of Ion Channels: A Variety of Functions for a Shared Structure

STEPHAN KELLENBERGER AND LAURENT SCHILD

Institut de Pharmacologie et de Toxicologie, Université de Lausanne, Lausanne, Switzerland

Kellenberger, Stephan, and Laurent Schild. Epithelial Sodium Channel/Degenerin Family of Ion Channels: A Variety of Functions for a Shared Structure. *Physiol Rev* 82: 735–767, 2002; 10.1152/physrev.00007.2002.—The recently discovered epithelial sodium channel (ENaC)/degenerin (DEG) gene family encodes sodium channels involved in various cell functions in metazoans. Subfamilies found in invertebrates or mammals are functionally distinct. The degenerins in *Caenorhabditis elegans* participate in mechanotransduction in neuronal cells, FaNaC in snails is a ligand-gated channel activated by neuropeptides, and the *Drosophila* subfamily is expressed in gonads and neurons. In mammals, ENaC mediates Na^+ transport in epithelia and is essential for sodium homeostasis. The ASIC genes encode proton-gated cation channels in both the central and peripheral nervous system that could be involved in pain transduction. This review summarizes the physiological roles of the different channels belonging to this family, their biophysical and pharmacological characteristics, and the emerging knowledge of their molecular structure. Although functionally different, the ENaC/DEG family members share functional domains that are involved in the control of channel activity and in the formation of the pore. The functional heterogeneity among the members of the ENaC/DEG channel family provides a unique opportunity to address the molecular basis of basic channel functions such as activation by ligands, mechanotransduction, ionic selectivity, or block by pharmacological ligands.

I. INTRODUCTION

The epithelial sodium channel (ENaC)/degenerin gene family represents a new class of ion channels that was discovered at the beginning of the 1990s. The degenerin genes *deg-1* and *mec-4* were first identified from a genetic screen of the mechanosensory pathway of *Caenorhabditis elegans*. The name degenerin (DEG) comes from the cellular phenotype induced by mutations of the *deg-1* gene and other related genes that result in selective

degeneration of sensory neurons involved in touch sensitivity. At the time of the identification of the DEG gene family in *C. elegans*, a functional cloning strategy in *Xenopus laevis* oocytes allowed the isolation and sequencing of a cDNA encoding the α-subunit of the amiloride-sensitive epithelial Na^+ channel ENaC (found in databanks under SCA, "sodium channel, amiloride sensitive," and SCNN1, "sodium channel, nonneuronal"). This channel was already known to play a crucial role in Na^+ absorption in the distal part of the kidney tubule and to be the target of aldosterone action. ENaC and degenerins were found to have substantial sequence homology. Additional members that formed a new subfamily within this emerging ion channel family were subsequently identified by sequence homology and characterized by functional expression. These related genes were found to be expressed mainly in the central and peripheral nervous system and were called mammalian degenerins (MDEG) or brain Na^+ channels (BNaC, BNC). After the discovery of their activation by extracellular protons these channels were named acid-sensing ion channels (ASICs). At about the same time the FMRF-amide-gated ion channel (FaNaC) was cloned from the mollusk *Helix aspersa*. This channel forms its own subfamily within the ENaC/DEG family of ion channels.

In contrast to channels that appeared at an early stage of evolution such as potassium, chloride, or water channels, ENaC/DEG genes are present only in animals (metazoa) with specialized organ functions for reproduction, digestion, and coordination. The members of the ENaC/DEG gene family show a high degree of functional heterogeneity that is unusual among the known gene families of ion channels. Their wide tissue distribution that includes transporting epithelia as well as neuronal excitable tissues best reflects the functional heterogeneity of the ENaC/DEG family members. Depending on their function in the cell, these channels are either constitutively active like ENaC or activated by mechanical stimuli as postulated for *C. elegans* degenerins, or by ligands such as peptides or protons in the case of FaNaC and ASICs. The evolution of the ENaC/DEG gene family certainly followed quite divergent paths to finally achieve a variety of different functions in the cell.

This review summarizes our present knowledge of the fundamental roles of the ENaC/DEG proteins and the relationship between their biophysical properties and structural characteristics. Despite their different functions in the cell, the members of the ENaC/DEG family retain common functional characteristics. Other recent reviews cover relevant aspects of ENaC/DEG family members in more detail than this review: amiloride-sensitive channels in epithelia (87), molecular mechanisms of human hypertension (153, 209), taste reception (155, 156), nociception (131, 175, 269), touch sensation in *C. elegans* (82, 243), and mechanotransduction (70, 88, 102).

II. PHYLOGENETIC AND SEQUENCE COMPARISON

Figure 1 shows a phylogenetic tree of the most relevant ENaC/DEG sequences available to date. Seven different branches can presently be distinguished in this gene family: the three main subfamilies comprise the SCNN1 genes encoding the ENaC α-, β-, γ-, and δ-subunits; the *C. elegans* degenerins (UNC, MEC, DEG, DEL);

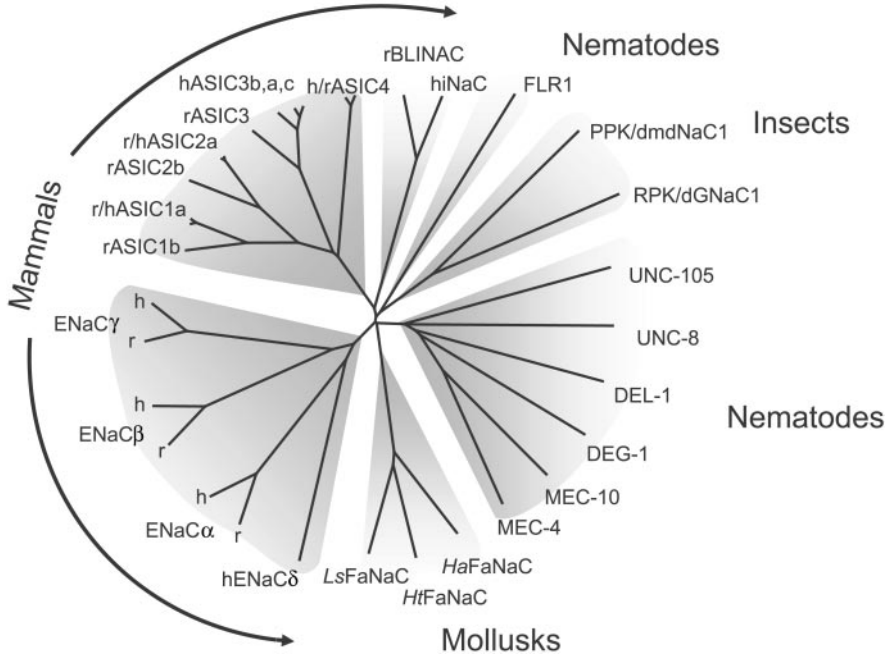

FIG. 1. Phylogenetic tree of the epithelial sodium channel (ENaC)/degenerin (DEG) family showing the organization into subfamilies of related sequences. Sequences were aligned by using the ClustalW algorithm. The channels from vertebrates are divided into three groups: ENaC, acid-sensing ion channels (ASICs), and brain-liver-intestine sodium channel (BLINaC)/human intestine sodium channel (hINaC). ENaC/DEG proteins of invertebrates can be divided into four groups: *1*) the degenerins from *Caenorhabditis elegans*; *2*) the *Drosophila* channels RPK/dGNaC1 and PPK/dmdNaC1; *3*) FMRFamide-gated sodium channel (FaNaC), which is expressed in mollusks; and *4*) FLR-1, which is the only characterized member of a group of *C. elegans* ENaC/DEG family members that are different from the degenerins.

and the ASICs. Smaller subfamilies found in invertebrates include the *Drosophila* proteins RPK/dGNaC1 and PPK/dmdNaC1, the peptide-gated Na^+ channel FaNaC of mollusks, and FLR-1 in *C. elegans* that is clearly distinct from the degenerins (171). The mammalian BLINaC (brain-liver-intestine amiloride-sensitive Na^+ channel) and hINaC (human intestine Na^+ channel) genes encode Na^+ channels that are clearly distinct from ENaC. The amino acid sequence identity between the different ENaC/DEG subfamilies is ~15–20%, whereas the identity within subfamilies is ~30% for the different ENaC subunits; ~30% for degenerins; 45–60% between the four ASIC genes ASIC1, ASIC2, ASIC3, and ASIC4; 38% for the two characterized *Drosophila* members; and ~65% for the three FaNaC orthologs. Within the ENaC subfamily two branches can be distinguished, one leading to the α- and δ-subunits and the other to β- and γ-subunits. The ENaC genes have been cloned from various species such as rat, human, cow, mouse, and *Xenopus laevis*, and for the sake of clarity, only human and rat sequences were used for the phylogenetic tree in Figure 1. The homology between human and rat orthologs of ENaC subunits is ~85%, and it is close to 100% between human and rat orthologs of ASIC1, ASIC2, and ASIC4 and ~83% for ASIC3. The hINaC and BLINaC genes share 79% sequence identity, and hINaC is probably the ortholog of the rodent BLINaC.

ENaC (47, 54, 142, 151, 247) and ASIC genes (see below) have different splice variants. For ASIC channels the nomenclature remains somewhat confusing in the literature. Initially ASICs were considered as the homologs of the degenerins because of their distribution in the central nervous system (CNS), and they were named mammalian degenerins (MDEG). The phylogenic tree however shows that the DEG and ENaC subfamilies are equally distant from the ASIC subfamily (Fig. 1); therefore, the name *mammalian DEG* for ASIC is phylogenetically incorrect. We use here a unified nomenclature adapted from Waldmann and Lazdunski (267). The ASIC subfamily comprises the following members: ASIC1a (also known as BNaC2, Refs. 83, 264), ASIC1b (or ASICβ, Refs. 18, 40), and additional splice variants of ASIC1 (40, 252), ASIC2a (or MDEG, MDEG1, BNC1, BNaC1, Refs. 83, 201, 266, 268), ASIC2b (MDEG2, Ref. 158), ASIC3 (or DRASIC, hTNaC1, Refs. 13, 61, 116, 263), and ASIC4 (or SPASIC, Refs. 7, 97).

The degenerin subfamily comprises only 6 members out of the 23 predicted ENaC/DEG proteins identified in the *C. elegans* genome (171, 246). FLR-1 is the only characterized member of a subfamily of eight members that can be defined by the presence of a conserved region in the extracellular domain related to, but distinct from, degenerin CRDII (171). FLR-1 is expressed in the *C. elegans* intestine and appears to be also functionally distinct from the degenerins (126, 134, 241).

Sequencing of the *Drosophila* genome identified 24 putative proteins related to the ENaC/DEG family (162), but so far only the two gene products Ripped Pocket (RPK/dGNaC1) (3, 55) and Pickpocket (PPK/dmdNaC1) (3, 56) have been characterized with regard to their function and/or tissue distribution.

The first draft sequence of the human genome reveals the presence of 11 proteins that can be assigned to the ENaC/DEG family: α-, β-, γ-, and δ-ENaC, ASIC1, -2, -3, and -4, and two or three proteins related to hINaC (256). Thus, at the present state of completion of the human genome, it seems unlikely that the number of mammalian genes encoding ENaC/ASIC proteins will greatly expand. It is interesting that no mammalian orthologs of the *C. elegans* DEG or FLR-1 genes, the *Drosophila* RPK/dGNaC1 and PPK/dmdNaC1 genes or of FaNaC have yet been identified in the human and the mouse genomes. This might indicate a divergence of the different ENaC/DEG subfamilies early in evolution.

III. PHYSIOLOGICAL ROLE

A. ENaC

The ENaC is located in the apical membrane of polarized epithelial cells where it mediates Na^+ transport across tight epithelia. In contrast to other Na^+-selective channels involved in the generation of electrical signals in excitable cells, the basic function of ENaC in polarized epithelial cells is to allow vectorial transcellular transport of Na^+. This transepithelial Na^+ transport through a cell basically involves two steps as illustrated in Figure 2. The large electrochemical gradient for Na^+ existing across the apical membrane provides the driving force for the entry of Na^+ into the cell. Active Na^+ transport across the basolateral membrane is accomplished by the Na^+-K^+-ATPase.

The apical entry of Na^+ is blocked by submicromolar concentrations of amiloride. The ENaC-mediated electrogenic Na^+ absorption in the distal nephron creates a favorable electrochemical driving force for K^+ secretion into the tubule lumen. This active transepithelial transport of Na^+ is important for maintaining the composition and the volume of the fluid on either side of the epithelium. In the kidney and the colon, which are target tissues for aldosterone action, the transepithelial sodium transport is crucial for the maintenance of blood Na^+ and K^+ levels and their homeostasis. In the lung or in salivary glands, Na^+ transport is certainly not important for the whole body Na^+ homeostasis, but rather for keeping the composition and the volume of the luminal fluid, i.e., the saliva or the alveolar fluid constant.

1. Kidney

In the kidney, ENaC is expressed in the distal nephron where sodium reabsorption is controlled by the

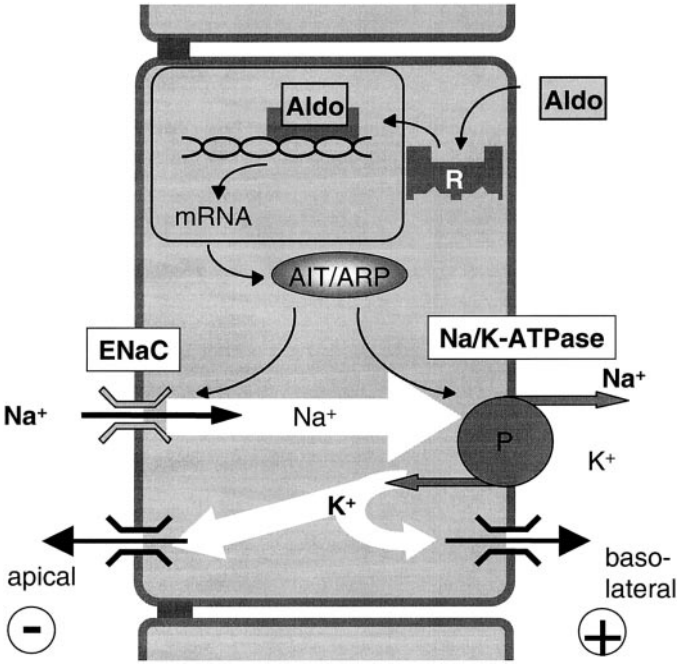

FIG. 2. Transepithelial ion transport in a principal cell of the cortical collecting duct (CCD). ENaC mediates Na^+ entry from the tubule lumen at the apical membrane, and the Na^+-K^+-ATPase extrudes Na^+ at the basolateral side. K^+ channels are present on the basolateral and apical membranes. K^+ channels at the apical membrane mediate K^+ secretion into the tubular lumen. The diagram also illustrates the action of aldosterone (Aldo) which binds to intracellular receptors that are translocated to the nucleus and affect the expression and subcellular localization of ENaC and the Na^+-K^+-ATPase as well as other target proteins via aldosterone-induced transcripts (AITs) and aldosterone-repressed transcripts (ARTs).

mineralocorticoid hormone aldosterone. In the distal nephron, Na^+ reabsorption can be measured in in vitro microperfused tubules as a large amiloride-sensitive Na^+ flux in sodium-deprived or aldosterone-treated animals (41, 204, 221). The first descriptions of the amiloride-sensitive Na^+ current at the single-channel level using the patch-clamp technique were obtained from principal cells of microdissected cortical collecting ducts (CCDs) (190) and from a cell line derived from the distal nephron of amphibians that responds to aldosterone (104). The presence of the amiloride-sensitive Na^+ current correlates with the expression of ENaC both at the mRNA and protein levels in the distal convoluted tubule, the connecting tubule, the CCD, and the outer medullary collecting duct. There is a clear axial heterogeneity of ENaC expression along the distal nephron; expression of ENaC is higher in superficial cortical regions of the distal nephron such as the connecting tubule or the CCD than in the deeper medullary regions such as the inner medullary collecting duct (IMCD) (69, 167, 168, 173, 260). In the CCD ENaC colocalizes with the water channel aquaporin-2, both being stimulated by vasopressin in this nephron segment (166). An electrogenic Na^+ transport sensitive to aldosterone is important in amphibian bladder and has also been found in the bladder of some mammals (150).

Under physiological conditions of hydration and salt balance, Na^+ reabsorbed in the distal nephron represents only a small fraction (<5%) of the filtered load. However, Na^+ reabsorption in the distal nephron can increase considerably in response to aldosterone or vasopressin secretion that is stimulated by dehydration and/or salt deprivation. This hormonal control is essential for the fine-tuning of Na^+ reabsorption in the distal nephron and the maintenance of sodium and fluid balance (208). The physiological and pathophysiological role of ENaC in Na^+ and K^+ homeostasis has been clearly demonstrated in human genetic studies and later confirmed by disruption of ENaC genes in mouse models by homologous recombination. Mutations in the β- and γ-ENaC genes causing hyperactive channels have been found in patients with Liddle's syndrome (105, 106, 114, 152, 218). Liddle's syndrome is a rare hereditary form of hypertension characterized by low plasma aldosterone levels and a low renin activity often associated with hypokalemia and/or metabolic alkalosis. These clinical features reflect an abnormally high Na^+ reabsorption in the distal nephron leading to expansion of the extracellular fluid volume and to the development of arterial hypertension. The insertion of a mutation causing Liddle's syndrome in the mouse β-ENaC gene locus by homologous recombination generated a mouse with a phenotype milder than the Liddle's syndrome in humans with extracellular volume expansion, high blood pressure associated with metabolic alkalosis, and hypokalemia that become evident only when animals are challenged with a high-salt diet (199). The elucidation of the genetic basis of Liddle's syndrome demonstrated the critical role of ENaC in maintaining a balance between the Na^+ intake and Na^+ excretion by the kidney (see Ref. 153 for review). The role of ENaC in Na^+ homeostasis was further evidenced by the identification of mutations in ENaC causing reduced channel activity or complete loss of channel function associated with pseudohypoaldosteronism type 1 (PHA-I) (39). The renal symptoms of this heterogeneous syndrome include hyponatremia, hypotension, and hyperkalemia and are associated with elevated plasma aldosterone and renin levels. Mouse models for PHA-I were obtained by different gene targeting strategies leading to decreased expression of α- or β-ENaC genes (112, 198) or complete knockout of the α-, β-, or γ-ENaC gene (15, 111, 176). The renal symptoms of these PHA-I mice were similar to those of the PHA-I patients, with a renal loss of sodium associated with hyperkalemia despite elevated plasma aldosterone levels. The physiological consequences of ENaC gene targeting in these animal models confirmed the critical importance of the three genes α-, β-, and γ-ENaC for channel function and Na^+ absorption in the distal nephron.

2. Lungs

The airway epithelia absorb Na^+ via an amiloride-sensitive electrogenic transport. This active Na^+ absorption is important for the maintenance of the composition of the airway surface liquid. The expression of the ENaC subunits along the respiratory epithelium is complex and varies between species. In adult rats and humans, the α-, β-, and γ-ENaC subunits are highly expressed in small and medium-sized airways (30, 74, 242). The α- and γ-subunits but not the β-subunit are expressed more distally in the lung, which may well correspond to a localization in the type II alveolar cells. This heterogeneity of the expression of ENaC subunits along the airways suggests differential regulation of liquid absorption by channels of various subunit compositions.

At birth the amiloride-sensitive electrogenic Na^+ transport is important to clear the liquid that fills the alveoli and the airways of the fetal mouse lung. mRNAs for α-, β-, and γ-ENaC can be detected in the fetal lung around *days 15–17* of gestation, and expression of ENaC subunits (mainly α- and γ-ENaC) sharply increases in the late fetal and early postnatal life when the lung turns from a secretory to an absorptive organ (242). The physiological role of ENaC in lung liquid balance was clearly demonstrated in mice in which the α-ENaC gene was inactivated by homologous recombination (111). These α-ENaC knock-out mice die soon after birth from respiratory failure due to a severe defect in the clearance of the fetal liquid that fills the lungs. These studies suggest that at birth α-ENaC in the mouse fetal lung is essential for Na^+ absorption. The disruption of the β- and γ-ENaC gene loci results in a slower clearance of the fetal lung liquid at birth but does not severely affect the blood gas parameters. The β- or γ-ENaC knockout mice die slightly later than the α-knockout from severe electrolyte imbalance, namely, hyperkalemia due to deficient renal K^+ secretion (15, 176). Thus, in contrast to the kidney, the Na^+ transport in the lung can be maintained efficiently by only two functional ENaC genes, i.e., the pairs α-β or α-γ.

In humans the contribution of α-ENaC to the clearance of fetal lung liquid at birth is still unclear. Very premature infants with respiratory distress syndrome have a reduced sodium absorption across the respiratory epithelia, as demonstrated by a reduced nasal transepithelial potential difference, likely contributing to the pathogenesis of this syndrome (14). However, PHA-I patients with severe disruption of the α-ENaC gene leading to near-complete channel loss of function have no report of respiratory distress syndrome at birth but show a more than twofold higher liquid volume in airway epithelia than normal individuals (139). Thus ENaC function in humans does not seem to be limiting at birth for the liquid clearance in the mature fetal lung. Differences between species in maturation of the lung, in mucociliary clearance, or in ENaC subunit expression in the respiratory epithelium may account for the phenotypic differences between human and mice.

3. Gastrointestinal tract and skin

In salivary glands, α-, β-, and γ-ENaC are detected at the RNA and protein levels in the apical membrane of the striated and interlobular ducts (69). An amiloride-sensitive Na^+ conductance has been described in mandibular duct cells using the whole cell patch-clamp technique (63). The IC_{50} of amiloride inhibition was ~5 μM, thus ~50 times higher than the IC_{50} of ENaC. The functional characteristics of this amiloride-sensitive current still await more detailed characterization to ascertain the functional contribution of ENaC in mediating Na^+ reabsorption in salivary glands.

The colon is a tight epithelium and an important site for Na^+ absorption. Part of this Na^+ transport is electrogenic, sensitive to amiloride and stimulated by aldosterone (71). Initially, the α-, β-, and γ-ENaC cDNAs were isolated from a rat distal colon cDNA library because of the high level of channel expression in this tissue (31, 33, 159).

The classical model of transepithelial Na^+ transport in tight epithelia (144) was originally described by Koefoed-Johnson and Ussing in the skin of amphibians and postulated the presence of an apical Na^+ channel and a basolateral Na^+-K^+-ATPase in series. The Na^+ transport in the amphibian skin responds to aldosterone with simultaneous morphological changes (261). In mammals, the three ENaC subunits are expressed in keratinocytes of all epidermal layers as well as in epithelial cells of hair follicles and sweat glands (210). ENaC transcripts can also be found in the pluristratified epithelium of the esophagus where ENaC's role is unknown (74). In sweat glands ENaC likely controls Na^+ excretion as in the kidney, but in the epidermis and hair follicles, the physiological role of ENaC is less clear. There is still no clear evidence for an ENaC-mediated transcellular Na^+ transport in mammalian epidermal cells, despite the presence of a benzamil-sensitive current in cultured human keratinocytes consistent with ENaC activity (29). Interestingly, expression of the α- and β-ENaC subunits is upregulated in cultured keratinocytes during differentiation, suggesting that ENaC may play a role in epidermal differentiation and skin development. Alternatively, this upregulation might be indirectly linked to the regulation of cell volume during this process (29, 183).

Finally, salt taste is transduced by direct amiloride-sensitive influx of Na^+ in the taste cells of the fungiform papillae of the anterior part of the tongue, suggesting the presence of an amiloride-sensitive Na^+ channel (for review, see Refs. 155, 156). The three α-, β-, and γ-ENaC subunits are expressed in the taste receptor cells of the

fungiform papillae (147, 154). The specific role of ENaC in salty taste transduction still remains to be clearly demonstrated, since the amiloride-sensitive inward currents recorded from whole taste receptor cells show lower affinity for amiloride and a lower single-channel conductance than expected from a typical ENaC current as estimated from noise analysis (9, 10).

4. Other tissues

The δ-ENaC subunit, closer to α- than to β- and γ-ENaC in its amino acid sequence, has been identified by sequence homology (Fig. 1). As expected from its close homology to α-ENaC, the δ-ENaC subunit can substitute for α-ENaC to form functional amiloride-sensitive Na^+ channels. The δ-ENaC subunit is expressed in testis, ovary, pancreas, and to a lesser extent in brain and heart (265). In the pancreas as in the ducts of salivary glands, an amiloride-sensitive channel might be responsible for Na^+ reabsorption. In the other tissues expressing δ-ENaC, amiloride-sensitive Na^+ currents have not yet been detected, and therefore, the physiological role of δ-ENaC in these tissues remains unknown.

The membranous labyrinth of the cochlea is a complex sensorineural epithelium. The basolateral side is bathed with the perilymph of similar ionic composition as the plasma or as cerebrospinal fluid. The endolymph at the apical surface of the membranous labyrinth is a K^+-rich, hyperosmotic fluid almost devoid of Na^+. The endolymph bathes the hair bundles of the sensory cells, and its ionic composition is critical for mechanotransduction. The α-, β-, and γ-ENaC subunit mRNAs are detected in the rat cochlea in both epithelial and nonepithelial structures (53). Interestingly, expression of the three ENaC subunits was strongest in epithelial cells (Claudius cells in particular) lining the scala media. The Claudius cells might be responsible for Na^+ reabsorption from the endolymph; the unusually high potential difference existing across the apical membrane of these cells (+80 mV in the endolymph and −100 mV intracellular) allows absorption of Na^+ from the endolymph at lower than millimolar concentrations (99). Furthermore, the mRNA abundance of the α-, β-, and γ-ENaC subunits in the cochlea increases during the first 10 days of life when the high-K^+, low-Na^+ composition of the endolymph is established. This observation suggests that ENaC in the epithelial cells of the scala media is critical for Na^+ extraction from the endolymph. However, no severe hearing problems have been reported for PHA-I patients with loss-of-function mutations of ENaC.

ENaC transcripts and proteins were detected in retina photoreceptors, but ENaC's role in phototransduction remains to be established (89). Finally, the γ-ENaC subunit has been localized in baroreceptor nerve termini innervating the carotid sinus (67). Structures specialized in mechanosensation in nerve endings of the rat footpad also express β- and γ-ENaC, and it was proposed that ENaC subunits represent components of mechanoreceptors for touch or blood pressure sensing (66). An involvement of ENaC in mechanotransduction has not yet been directly demonstrated.

B. ASICs

ASICs were cloned based on their homology to ENaC/DEG channels (for a recent review, see Ref. 267). Four ASIC genes (ASIC1–4) have been identified, and three of them exist in different splice variants (Fig. 1, see sect. II). The expression of ASIC mRNAs has been analyzed by Northern blotting and in situ hybridization (26, 267) and shows a high expression in the nervous system. ASIC1a, ASIC2a, and ASIC2b have a similar widespread distribution pattern in the brain, with the highest expression levels in the hippocampus, the cerebellum, the neo- and allocortical regions, the main olfactory bulb, the habenula, and the basolateral amygdaloid nuclei. Coexpression with ASIC4 is found in many areas of the brain (7, 97). In addition, strong expression of ASIC4 has been found in the pituitary gland (97).

In the peripheral nervous system, the ASIC channels are found predominantly in small-diameter sensory neurons involved in pain sensation (40). Rat ASIC3 is expressed almost exclusively in sensory neurons (12, 13, 40, 263). ASIC3 is expressed in sympathetic cardiac afferents that innervate the heart where they may play a role as mediators of cardiac pain (23, 240). Expression of ASIC2a in sensory neurons is lower compared with other ASICs (158, 200). ASIC2a is also found in the taste buds of the circumvallate papillae where it may have a function in sour taste perception (250). ASIC2b has to date only been found in the rat. As for ENaC subunits, ASIC4 expression was demonstrated in the inner ear, but its role in hearing function remains to be established (97).

ASIC channels are activated by a drop of the extracellular pH. Expression of homomultimers or heteromers of ASIC1–3 in heterologous cell systems generates proton-gated cation currents with functional properties resembling the native currents found in sensory and CNS neurons and in oligodendrocytes (25, 92, 148, 164, 255, 267). The magnitude of these depolarizing H^+-gated currents is sufficient to initiate action potentials in neurons (72, 255). So far, no channel function has been found for ASIC4 (7, 97).

The physiological role of ASICs remains uncertain. Their expression in sensory neurons suggests a role in pain perception following tissue acidosis (203, 263, 267). For instance, good electrophysiological evidence supports the involvement of ASIC3 in cardiac ischemic pain sensation (23, 240). Myocardial extracellular pH drops to

6.7 during severe cardiac ischemia, a pH value that can evoke a high-amplitude current in the sympathetic cardiac afferents expressing ASIC3 (240). This current shows the same functional characteristics as the H^+-gated current in COS-7 cells expressing ASIC3 (240). Amiloride that blocks ASICs with low affinity has recently been shown to have analgesic effects in a variety of animal pain models (75). This finding however has to be interpreted with some caution because at concentrations at which amiloride blocks ASICs, it also blocks other channels and proteins in the brain, as, e.g., voltage-gated Ca^{2+} channels (143). Finally, nonsteroid anti-inflammatory drugs inhibit ASIC currents (259). The potential involvement of ASICs and other ion channels in pain sensation has been reviewed (131, 175, 269).

In the CNS, tissue acidosis is a well-established feature of cerebral ischemia which aggravates cell damage (reviewed in Ref. 161). Transient global ischemia induces expression of ASIC2a protein in neurons that survive ischemia (129). ASICs may also be involved in controlling neuronal activity associated with external pH fluctuations (44). A significant acidification of the extracellular space has been found to be associated with repetitive stimulation and epileptiform activity (43, 44, 233, 253, 270). Recently, it has been shown that expression levels of ASIC1a and ASIC2b (but not ASIC2a) decrease in specific brain regions in the pilocarpine model of epilepsy (26). The question remains if in vivo extracellular pH changes are large enough to activate ASIC channels. It is possible that under physiological conditions endogenous ligands of ASICs such as Zn^{2+} or FMRFamide-related peptides may facilitate activation (8, 16).

ASIC2 knockout mice (200) had normal appearance, growth, size, temperature, fertility, and life span, with no obvious defects in pain sensation. The only phenotype that could be detected in an in vitro skin-nerve preparation from ASIC2$^{-/-}$ mice was a reduced sensitivity of a specific component of mechanosensation, involving the low-threshold rapidly adapting mechanoreceptors. In rodent hairy skin, these mechanoreceptors are excited by hair movement. Consistent with this function, ASIC2a/b was found in the lanceolate nerve endings that lie adjacent to and surround the hair follicle. In a recent immunocytochemical study, expression of ASIC2a was found in specialized cutaneous mechanosensory nerve terminals (86). The relatively discrete phenotype due to ASIC2 loss of function could be due to a redundancy of ASIC proteins in the formation of heteromultimeric channels.

C. Degenerins

Mechanosensory transduction refers to processes that convert mechanical forces into bioelectrical signals. Mechanotransduction is important for different physiological functions such as touch, hearing, or proprioception. The extensive genetic dissection of mechanosensory behavior in *C. elegans* led to the identification of a number of genes involved in the development, survival, function, and regulation of touch receptor neurons (37). Among these genes, the degenerins that form a subgroup of the ENaC/DEG family play a critical role in touch sensation and proprioception.

Specific mutations in MEC-4, MEC-10, UNC-8, UNC-105, or DEG-1 cause swelling and subsequent death of the cells in which the mutant proteins are expressed. These proteins were called degenerins because of the cell degenerative phenotype they cause when mutated (reviewed in Refs. 171, 243). Typical morphological features involved in this phenomenon include the production of membrane infoldings, membrane whorls, and vacuoles that resemble those found in excitotoxic cell death after ischemia, hypoxia, or epilepsy. The initial response of the cell is an enhanced membrane cycling that may reflect attempts to dilute or to sequester harmful components localized to various membranes and to translocate them to degradative vacuoles (101). On the basis of their homology with ENaC, it has been proposed that these degenerins function as mechanosensory channels which when mutated become hyperactive leading to increased cation influx into the cell and to cell death.

Mechanotransduction in *C. elegans* has been described in detail in several recent reviews (82, 171, 243). When a *C. elegans* moving over an agar plate is gently touched with an eyelash hair on the posterior part of the body, the animal will move forward, and when touched on the anterior body, it will move backward. This gentle touch is sensed by six touch receptor neurons. Their processes run longitudinally along the body wall on the ventral and both lateral sides and are embedded in the hypodermis (the "worm skin"), to which they appear to be glued by an extracellular material called the mantle (reviewed in Refs. 82, 243). The position of the processes along the body axis correlates with the sensory field of the touch cells.

Genetic analysis has identified 16 genes which, when mutated, specifically disrupt gentle body touch sensation; they represent, therefore, candidate mediators of touch sensitivity. These genes were named *mec* genes because when defective the animals become "mechanosensory abnormal." Many of the *mec* genes have been molecularly identified, and the encoded proteins were postulated to form a touch-transducing complex that converts the mechanical stimuli into an electrical signal. Only some of the *mec* genes belong to the ENaC/DEG family such as MEC-4 (243) or MEC-10 expressed in the touch receptor neurons (110).

The transduction of mechanical stimuli into bioelectrical signals requires activation of an ion channel to generate an ionic current. So far, functional expression

experiments have failed to demonstrate mechanically inducible channel activity. Constitutively active channels were obtained after coexpression of MEC-4 and MEC-10 with the stomatin-related protein MEC-2 (Fig. 4) or upon expression of UNC-105 containing activating mutations (84, 90). However, the mechanosensitivity of these degenerins still remains to be demonstrated in heterologous expression systems.

UNC-8 (*unc* stands for uncoordinated) is expressed in several sensory neurons, interneurons, and the motorneurons VA and VB (245). This subclass of motorneurons shows the peculiar neuroanatomical feature of having their synapses with the muscle or the interneurons restricted to a limited region close to the cell body. Similar anatomical features are found in corresponding motorneurons in the nematode *Ascaris suum* that are known to be stretch responsive, suggesting that VA and VB motorneurons in *C. elegans* have similar functions (57). The degenerins UNC-8 and DEL-1 are coexpressed in the ventral cord VA and VB motorneurons. Functional evidence for involvement of UNC-8 in modulation of locomotion comes from observation of wild-type and UNC-8 mutant animals. When moving on agar plates, wild-type worms inscribe a sinusoidal wave. In *unc-8* null mutants, the amplitude is reduced by ~3.5-fold (245). It has been proposed that the contribution of UNC-8 to modulation of nematode locomotion relies on feedback information on body posture, thus on an activity that is related to proprioception (243, 245). Alternatively UNC-8, which is also expressed in interneurons that regulate locomotion, might act within these neurons to modulate coordinated movement. The only evidence for the involvement of DEL-1 in modulation of *C. elegans* locomotion lies in its coexpression with UNC-8 in the VA and VB motorneurons and its homology to other ENaC/DEG family members (243, 245). Like MEC-4 and MEC-10, UNC-8 and DEL-1 are thought to form the ion channel core of the stretch-sensitive complex mediating modulation of *C. elegans* locomotion.

Yet another member of the *C. elegans* degenerin subfamily contributes to proprioception by monitoring muscle stretch. The UNC-105 gene is not expressed in neurons but in muscles. Mutations of the UNC-105 ENaC/DEG gene have been identified that create constitutively activated channels that cause muscle hypercontraction (163, 194), presumably because muscle cells are depolarized by an inappropriate cation influx through the UNC-105 channels. As mentioned above, expression of UNC-105 containing activating mutations in *Xenopus* oocytes results in ion channel activity, but mechanosensitivity of the UNC-105 channel has not been demonstrated (84).

D. *Drosophila* ENaC/DEG Members

Among the 24 predicted proteins of *Drosophila* related to the ENaC/DEG family (162), only Ripped Pocket (RPK/dGNaC1) (3, 55) and Pickpocket (PPK/dmdNaC1) (3, 56) have so far been characterized with regard to their function and/or tissue distribution. RPK/dGNaC1 transcripts are present exclusively in fly ovary and testis; they are maternally deposited into the embryo, where they persist until late gastrulation. The expression of RPK/dGNaC1 transcripts in *Drosophila* is restricted to oocytes in late vitellogenic stages and to early embryos, as well as to nurse and follicular cells. This suggests that RPK/dGNaC1 is involved in early development. When expressed in *Xenopus* oocytes RPK/dGNaC1 forms functional Na^+-selective channels with low apparent affinity for amiloride (see Table 1). It was not possible to record any RPK/dGNaC1 activity in transfected mammalian COS cells. This observation was interpreted as RPK/dGNaC1 activity being modulated by specific factors that are present only during early development and might therefore be present in oocytes but not in COS cells (55). Amiloride-sensitive Na^+ channels in mammalian embryos play an important role in fluid transport across the trophectoderm and in the formation of the blastocyst (3, 55). Like RPK/dGNaC1, these channels appear to have a low sensitivity to amiloride (K_i = 12 μM, Ref. 207). RPK/dGNaC1 and related members in *Drosophila* may play roles in fluid distribution and cell volume regulation during gametogenesis and early development.

The PPK/dmdNaC1 gene product appears at later developmental stages of *Drosophila*. It is expressed in sensory dendrites of a subset of peripheral neurons in late-stage embryos and early larvae. The late PPK/dmdNaC1 expression coincides with the end of elaboration of the nervous system, after the complete determination and differentiation of neuroprecursor cells. This led to the hypothesis that PPK/dmdNaC1 is not involved in the differentiation of the peripheral nervous system but rather in the function of PPK/dmdNaC1-expressing neurons (56). In insects, multiple dendritic neurons in which PPK/dmdNaC1 is expressed are thought to play a role in touch sensation and proprioception. For this reason, it has been proposed that in analogy to degenerins, PPK/dmdNaC1 may function as a mechanotransduction channel. PPK/dmdNaC1 does not produce functional ion channels when expressed in *Xenopus* oocytes (3, 56).

E. FaNaC

The FMRFamide (Phe-Met-Arg-Phe amide)-gated channel, or FaNaC, was originally cloned from a cDNA library from the snail *Helix aspersa* nervous system, based on its homology to ENaC/DEG family members.

TABLE 1. *Biophysiological and pharmacological properties of functionally expressed ENaC/DEG channels*

Name	Activator	P_{Na}/P_K	P_{Li}/P_{Na}	g_{Na}, pS	IC_{50} Amiloride, μM	IC_{50} Benzamil, μM	EC_{50} Activator, for H^+	Expression pH System	Reference No.
Unc-105	Degmut	1.8	0.93	4.6[a]	7.7/80[b]			X.o.	84
MEC-4/ MEC-10/ MEC-2	Degmut	>1	1.44		0.4			X.o.	90
RPK	Constitutive	>(>)10	~1		9–24	2		X.o.	3, 55
RPK	Degmut	≫10	1.12		0.45				3
FaNaC(Ha)[j]	FMRFamide	~5–10	0.7	9.2–13.1	0.6	0.2	FMRFa:2 μM	X.o.	157, 272
FaNaC(Ht)[j]	FMRFamide	ND	ND	6.8	[c]	[c]	FMRFa:70 μM	X.o.	127
ASIC1a	H^+	6–13	0.8	14.3	10	10	6.2–6.4	X.o., HEK, COS	240, 264
ASIC1b	H^+	~3			21		5.9	COS	40
ASIC2a	Constitutive	≥10	1		0.15			X.o.	201
ASIC2a[d]	Degmut	2.8–5.6		1.7–4.3	1.7–13	1.6–16		X.o., HEK	266
ASIC2a	H^+	10		10.4	28		4.35	X.o.	38
ASIC3 transient	H^+	5–12		13–15	60–100		6.5–6.7 (3.7)	COS (X.o.)	12, 13, 61, 240, 263
ASIC3 sustained	H^+	12			Partially blocked at 100 μM		3.5/4.3		12, 13, 263
ASIC1a/2a	H^+	7[e]	0.5/1[f]	10	20		4.8/5.7	X.o. COS	17, 59
ASIC2a/2b	H^+	~10[g]		13.7[a]			~4	COS	158
ASIC2a/3	H^+	≫1[e]			~100 (tr)[h]		4.3–4.6	X.o.	12
ASIC2b/3	H^+	~10[g]					6.5	COS	158
BLINaC	Degmut[i]	≥10	1.15	9.0–10.6	1.3	2.4		X.o. COS	212
hlNaC	Degmut	~8			0.5	0.8		X.o.	216
ENaC $\alpha\beta\gamma$	Constitutive	≥100	~1.6	4–5	0.1	0.01		X.o.	33, 137, 138, 220
ENaC $\alpha\beta$	Constitutive	≥100	0.8	5.1	4	0.4		X.o.	177
ENaC $\alpha\gamma$	Constitutive	≥100	1.5	6.5	0.13	0.015		X.o.	177
ENaC $\delta\beta\gamma$	Constitutive	>50	0.6	12	2.6	0.27		X.o.	265

Activator indicates how the ENaC/DEG channels were activated in the studies cited: degmut, activated by mutation of the pre-M2 degenerin site; X.o., *Xenopus* oocytes. [a] Several (sub)conductance levels found. [b] Channel activated by P134S/A692V mutation. [c] Amiloride and benzamil enhanced the FMRFamide response. [d] Analysis of several different degenerin mutants. [e] Similar for transient and sustained current. [f] Determined from current ratio/reversal potential. [g] Sustained current not Na^+/K^+ selective. [h] Slightly lower affinity for sustained current. [i] Wild-type gave tiny, nonselective currents. [j] FaNaC of *Helix aspersa* (Ha) and *Helisoma trivolvis* (Ht). ND, not determined.

FaNaC mRNA is detected in the nervous system and in pedal muscle of this snail (157). The biophysical and pharmacological properties of the cloned FaNaC expressed in *Xenopus* oocytes are very similar to those of the native FMRFamide-gated current in *Helix* neurons (51, 93, 94). FMRFamide induces a fast excitatory depolarizing response due to direct activation of the channel in neurons of the snail *Helix aspersa* as well as in *Aplysia* motor neurons (19, 94, 211). This fast response is readily distinguished from other, slower neuronal FMRFamide responses in *Helix aspersa* (reviewed in Ref. 51) that depend on G proteins. Evidence that the peptide directly gates a channel was obtained using isolated membrane patches from the *Helix* C2 neuron and from *Xenopus* oocytes expressing the cloned FaNaC. Inward unitary currents could be generated by external application of FMRFamide to excised outside-out patches when G protein-mediated responses were inhibited (94, 157). This finding represented the first functional description of a peptide-gated ion channel. Recently, the cDNAs encoding FMRFamide-gated channels from two other mollusks, *Helisoma trivolvis* and *Lymnaea stagnalis*, were cloned (127, 196). These different clones share 60–65% identity of the amino acid sequence. So far, no mammalian homologs of FaNaC have been identified (8, 256), but FMRFamide and the mammalian neuropeptide FF as well as related peptides can modulate the activity of ASICs in heterologous expression systems (8).

IV. STRUCTURAL ASPECTS

A. Primary Structure and Membrane Topology

The size of the ENaC/DEG proteins ranges from ~530 to ~740 amino acids. Regions of conserved amino acid sequences in ENaC/DEG family members are likely to represent structural elements important for channel function. These conserved domains shown in Fig. 3, *A* and *B*, are located essentially in the transmembrane segments and their proximity and in the extracellular loop.

A few sequences are completely conserved among the ENaC/DEG family members; they include a HG motif (His-Gly) located in the NH_2-terminal cytoplasmic domain in close proximity to the M1 segment, a FPxxTxC sequence following M1 (post-M1) and completely conserved residues in the M2 region. The extracellular loop contains cysteine-rich domains (CRD) II and III. The conserved

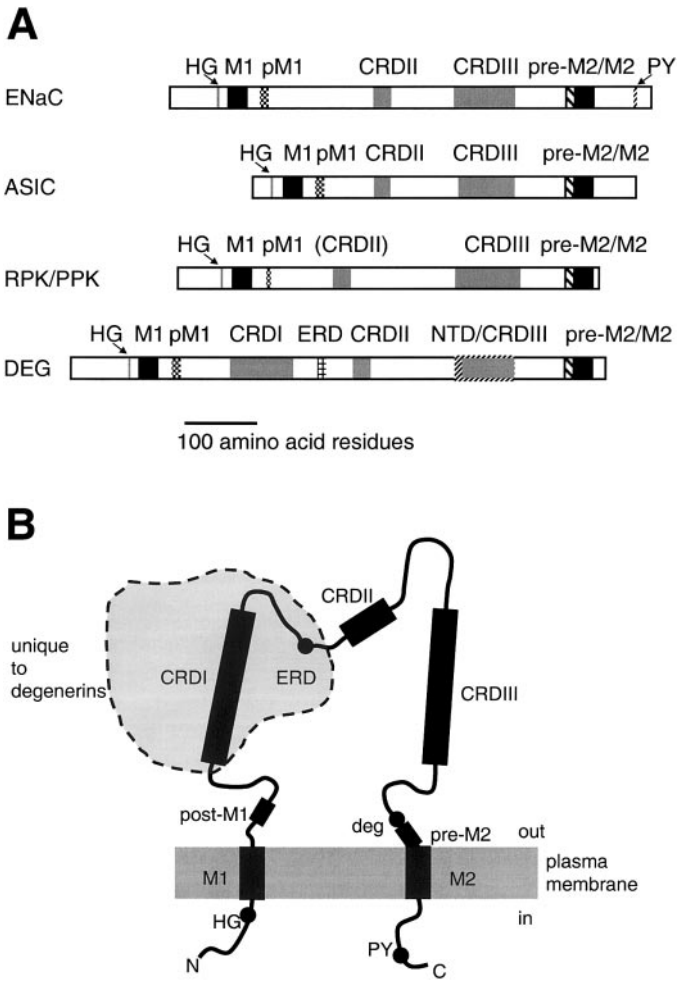

FIG. 3. Conserved domains and their localization in ENaC/DEG family members. *A*: linear representation of the primary structure shows the conserved regions found in each of the main subfamilies. The length of the domains in the diagram reflects their relative size in the protein. M1, M2, transmembrane segments; HG, conserved His-Gly motif within a conserved NH_2-terminal domain; pM1, post-M1, conserved domain directly downstream of M1; CRD, cysteine-rich domain; pre-M2, hydrophobic domain directly preceding M2; ERD, extracellular regulatory domain unique to *C. elegans* degenerins; NTD, neurotoxin domain (244); PY, PPPxY domain of α-, β-, and γ-ENaC. *B*: membrane topological organization of an ENaC/DEG subunit. The part that is unique to degenerins (containing CRDI and ERD) is shown on a gray background encircled by an interrupted line. Abbreviations are as in *A*. The residue in the pre-M2 domain whose mutation induces degeneration of the cells expressing these mutant degenerins is indicated as "deg."

Cys residues might be involved in the formation of disulfide bonds to maintain the tertiary structure of the large extracellular loop. Candidate cysteine residues in the extracellular loop of α-ENaC involved in disulfide bridges have been identified by tandem Cys mutations and functional analysis (77).

Other domains are conserved only within particular ENaC/DEG subfamilies. Two domains in the extracellular loop are conserved exclusively within the degenerin subfamily, the cysteine-rich domain CRDI and the extracellular regulatory domain ERD (85). ENaC subunits contain conserved proline-rich motifs in the cytoplasmic COOH terminus that are unique to the ENaC subfamily. These motifs have the consensus sequence PPPXYXXL and are involved in protein-protein interactions.

The membrane topology has been investigated essentially for ENaC, but we can assume from the overall sequence homology that this topology is shared by the other ENaC/DEG family members. Analysis of the membrane topology of ENaC was performed by protease digestion analysis of α-ENaC translated in vitro and reconstituted in microsomes (205). This analysis was consistent with M1 and M2 being separated by a large extracellular loop of ~50 kDa, the NH_2 and COOH termini being cytoplasmic. This large extracellular loop makes up more than one-half of the channel protein and represents a structural feature unique to the ENaC/DEG family members that is not found in other ion channel families. Several putative glycosylation sites are present in the extracellular loop of ENaC subunits (6 for α, 12 for β, and 5 for γ). Site-directed mutagenesis in α-ENaC showed that the six potential *N*-glycosylation sites between M1 and M2 but not the two putative *N*-glycosylation sites preceding M1 are used, demonstrating the extracellular topology of the loop between M1 and M2 (32, 230). In addition, with the use of truncated α-ENaC fused with the Na^+-K^+-ATPase β-subunit that is known to be glycosylated, it was demonstrated that M1 and M2 serve as start-transfer and stop-transfer signals, respectively, consistent with both M1 and M2 crossing the membrane and leaving the COOH terminus cytoplasmic (32).

The hydrophobic profile of ENaC subunits reveals a stretch of hydrophobic amino acid residues preceding M1 and M2. The protease digestion pattern of α-ENaC is consistent with the presence of a short segment preceding M2 that is accessible for the protease from the cytoplasmic side (205). In all known Na^+- or K^+-selective cation channels, the short hydrophobic segment preceding the most COOH-terminal transmembrane domain forms the outer pore of the channel with the receptor sites for external blockers. This analogy led to the suggestion that the pre-M2 segment of ENaC subunits may contribute to the formation of the channel pore.

B. Multimeric Channels and Subunit Stoichiometry

1. ENaC/FaNaC

The initial cloning experiments demonstrated that the three homologous ENaC subunits α, β, and γ are required for maximal expression of ENaC activity (33). Thus it became clear that the structure of ENaC is a heteromultimeric channel similar to the nicotinic acetylcholine receptor. There is presently good evidence that the three ENaC subunits contribute to the formation of the channel pore and line a unique ion permeation path-

way (137, 138, 220, 223, 231) (see sect. v). It should be mentioned that other models for the subunit arrangement around the channel pore have been proposed based on functional experiments with channels reconstituted in lipid bilayers. According to these models, ENaC shows a triple barrel organization to account for the different subconductance states of the channel reconstituted in lipid bilayers (22). Such models for ENaC have not gained any experimental support from functional studies in cellular expression systems such as the *Xenopus* oocyte.

The relative abundance of the three ENaC subunits at the cell surface in *Xenopus* oocytes expressing amiloride-sensitive Na^+ current was determined by quantitative analysis of the binding of radiolabeled antibodies directed against a FLAG epitope introduced into the extracellular domain of α-, β-, and γ-subunits (78). The low current expression after expression of α-ENaC alone is correlated with a low level of α-ENaC subunit expression at the cell surface, suggesting a retention of α-ENaC in the endoplasmic reticulum due to the absence of a molecular signal essential for targeting the channel to the cell surface. In oocytes expressing the three ENaC subunits α, β, and γ, the α-subunit is approximately two times more abundant in active ENaC channels at the cell surface compared with β- or γ-subunits (76). This 2:1:1 ratio of channel subunits remains constant even under conditions where one subunit is overexpressed relative to the two other homologous subunits (76), consistent with a preferred fixed subunit stoichiometry when the three ENaC subunits are available for channel assembly.

Despite the preferred subunit stoichiometry of ENaC, the α-, β-, and γ-subunits are to some extent interchangeable. Expression of α- or δ-ENaC alone in *Xenopus* oocytes has been shown to generate small amiloride-sensitive currents, suggesting that homomeric α-ENaC and δ-ENaC channels are functional. Expression of the ENaC subunit combinations α-β or α-γ generates a similar level of amiloride-sensitive current that is higher than after expression of α-ENaC alone, suggesting that β- and γ-subunits can replace each other in the channel complex (33, 78, 177). Early expression experiments in *Xenopus* oocytes indicated that β-γ channels were not expressed at the cell surface (33, 78). However, it has been later shown that 6 days after injection of cRNA encoding β- and γ-ENaC subunits a small but significant amiloride-sensitive current could be detected, suggesting that functional channels can be formed with β- and/or γ-subunits (27).

In the absence of high-resolution images, the determination of the number of subunits in the functional channel relies on a biochemical analysis of the channel complex at the cell surface. This approach was first performed on FaNaC because this channel is functional as a homomultimer. In addition, the mature FaNaC at the cell surface is fully glycosylated and thus biochemically identifiable. Following the maturation process and the oligomerization of the channel complex, Coscoy et al. (50) showed that the tetrameric assembly of the channel occurs already in the endoplasmic reticulum where this immature oligomeric complex is core glycosylated. Chemical cross-linking experiments were consistent with a minimal stoichiometry of four subunits, and the hydrodynamic characterization of the channel complex revealed a maximal number of five subunits (50).

Alternatively, the number of homologous subunits forming a channel can be assessed by the quantitative analysis of the contribution of each subunit to channel function. The identification of mutations in α-, β-, and γ-subunits that confer to the channel a resistance to block by amiloride or a sensitivity to block by Zn^{2+} allowed the design of experiments to assess for each of the three ENaC subunits the number of subunits per channel complex that contribute to a particular channel function (76, 220). These experiments followed the basic principles originally described to determine the subunit stoichiometry of the *Shaker* K^+ channel by studying the interaction of a toxin with channels made of different fractions of wild-type and toxin-resistant mutant subunits (170). The Zn^{2+} sensitivity of ENaC was conferred to the channel when the channel complex contained two α-subunits carrying a cysteine substitution at the amiloride binding site (76). Inversely, block by the sulfhydryl reagent 2-aminoethyl methanethiosulfonate (MTSEA) was conferred to the channel when at least one of two α-subunits carried the same cysteine substitution (146). These experiments were consistent with the presence of two α-ENaC subunits in the functional channel. The same approach using point mutations on β- or γ-ENaC that confer amiloride resistance did not provide any information about the absolute number of β- and γ-subunits, since the magnitude of the amiloride-resistant current was directly proportional to the fraction of mutant β- or γ-subunit expressed (76, 146).

In contrast to FaNaC, ENaC at the cell surface of *Xenopus* oocytes is not fully glycosylated, making a biochemical approach difficult for assessing the channel subunit stoichiometry. Subunit stoichiometry of ENaC can be assessed by expression of trimeric or tetrameric constructs made of α-, β-, and γ-ENaC subunits linked in a head-to-tail fashion. The rationale of this approach relies on the assumption that the correct concatameric construct does not need to be complemented by monomeric subunits for channel function (145). The analysis revealed that the α-β-α-γ construct is sufficient for the expression of functional channels and does not require complementation by additional monomeric subunits (76). Thus, taken together, the following observations support a tetrameric subunit organization around the channel pore, as illustrated in Figure 4*A*: *1*) the surface expression of α-ENaC per active channel is approximately two times higher than for β, *2*) there are consistently two α-subunits per active

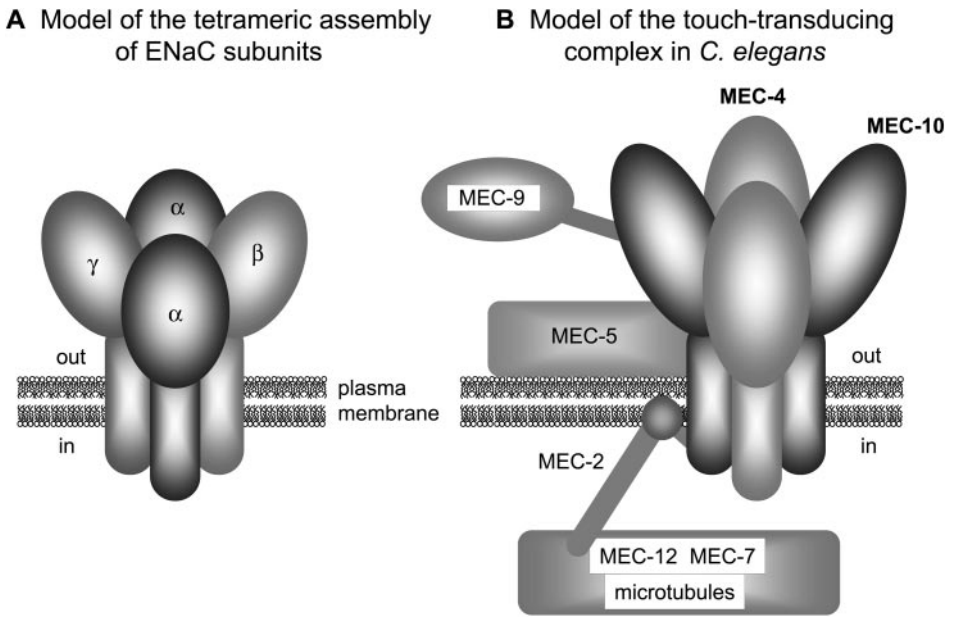

FIG. 4. Model of ENaC/DEG channel complexes. *A*: model of the tetrameric assembly of an ENaC channel. The model shows the tetrameric assembly of ENaC subunits around the central channel pore. The model is based on functional analyses that showed that all ENaC subunits participate in the formation of the channel pore and established the subunit stoichiometry (76). *B*: model of a touch-transducing complex in *C. elegans*. This model is based on genetic analysis. Touch transduction is thought to be mediated by a degenerin ion channel made of at least two MEC-4 (light gray) and two MEC-10 (dark gray) subunits. The large extracellular domains of the subunits project into a specialized extracellular matrix called the mantle, which includes the MEC-5 collagen and the MEC-9 protein. Inside the touch receptor neuron are special microtubules made up of the MEC-12 α-tubulin and the MEC-7 β-tubulin. The microtubules are proposed to be linked to the channel by means of stomatin-related MEC-2, a peripheral membrane protein. Proteins tethered to the extracellular and intracellular sides are thought to exert pressure on the channel, conferring gating tension when the channel is stretched between these two contact points. [Adapted from Mano and Driscoll (171).]

channel, *3*) the number of β- and γ-subunits are equal, and *4*) α-β-α-γ is the minimal concatameric construct for functional channel expression. This tetrameric subunit composition of ENaC is consistent with the subunit stoichiometry of other Na^+- or K^+-selective ion channels and in particular with the stoichiometry of channels made of subunits with two transmembrane domains.

With a similar approach looking at interactions of sulfhydryl reagents with ENaC wild-type and mutants together with the biochemical determination of the molecular mass of ENaC and FaNaCh, Snyder et al. (229) reached the conclusion that ENaC as well as other members of the ENaC/DEG gene family are made of nine subunits: three α-, three β-, and three γ-subunits in the case of ENaC. This nonameric channel stoichiometry was further supported by freeze-fracture electron microscopy in oocytes expressing ENaC (73). Such high-magnification images revealed particles of 8 nm in diameter compatible with ENaC channels. Based on the assumption that the cross-sectional area of membrane proteins in freeze-fracture microscopy is proportional to the number of the membrane-spanning domains, ENaC was found to have 17 membrane-spanning segments corresponding to 8 or 9 subunits. These conclusions should be taken with caution because the relationship between the cross-sectional area and the number of transmembrane segments is certainly not constant for all membrane proteins, and the functional ENaC channel complex may well include additional helical segments embedded in the membrane or associated proteins.

2. *Touch- and stretch-transducing complexes in* C. elegans *degenerins*

C. elegans degenerins are implicated in touch sensation and proprioception. Based on the genetic analysis of *C. elegans* mutants with impaired touch and stretch sensation, a model of the touch-transducing complex was proposed in which the degenerins MEC-4 and MEC-10 constitute the channel core of the mechanosensory transduction complex (see Fig. 4*B*) (70). MEC-4 and MEC-10 subunits are coexpressed in touch receptor neurons, and genetic interactions could be demonstrated between *mec-4* and *mec-10* (100, 110, 243). In *Xenopus* oocytes expressing MEC-4 and MEC-10, both proteins could be immunoprecipitated, suggesting the presence of functional heteromeric channels (90). The number of MEC subunits that form the channel pore has not yet been established, but genetic evidence is compatible with at

least two MEC-4 and two MEC-10 subunits per channel (108, 110).

Because mechanosensation could not be reconstituted in heterologous expression systems with MEC-4 and MEC-10 alone, additional associated proteins likely participate in the functional complex at the cell surface. Degeneration caused by mutations of a number of degenerins (*deg-1*, *mec-4*, *mec-10*, and *unc-8*) requires an additional gene, MEC-6, essential for activation of the mechanosensitive channel (reviewed in Ref. 243). MEC-6 has not been cloned yet and might encode a protein that mediates localization or posttranslational modification of the putative channel-forming subunits. In addition, MEC-2, a stomatin-related protein essential for touch sensation, is associated with the channel complex and increases channel activity in oocytes expressing MEC-4 and MEC-10 (90).

To sense mechanical stimuli, the large extracellular loops of MEC-4 /MEC-10 channels are postulated to be linked to the touch cell-specific extracellular matrix, by interaction with the MEC-5 collagen and/or MEC-9, a large protein rich in interaction domains such as epidermal growth factor (EGF)-like repeats (2 of them of the Ca^{2+}-binding type) and Kunitz protease inhibitor domains (68) (see Fig. 4*B*). The intracellular domains of MEC-4 and MEC-10 are hypothesized to be tied to the unique 15-protofilament microtubules (made of the MEC-12 α-tubulin and the MEC-7 β-tubulin) by the linker protein MEC-2, which is related to stomatin (reviewed in Ref. 243). By anchoring the channel on both sides of the membrane, displacement of the extracellular matrix with respect to the cytoskeleton is supposed to open the channel in response to mechanical stimuli. A model for the stretch-sensitive complex mediating proprioception similar to that of the touch-transducing complex has been proposed, containing UNC-8 and DEL-1 as subunits of the channel core in the mechanotransducing complex (243).

In summary, there is good evidence that *C. elegans* DEG subfamily members represent the channel subunits of a large mechanotransduction complex in the plasma membrane. The channel core of this complex is heteromultimeric and made of at least four DEG channel subunits belonging to the ENaC/DEG family. Other components might be involved in this mechanotransduction complex to anchor the channel to cell constituents on both sides of the membrane.

C. Genomic Organization

The human α-ENaC gene (SCNN1A) covers 17 kb on chromosome 12p13. The human β- and γ-ENaC genes (SCNN1B and SCNN1G) are located on chromosome 16p in very close proximity, suggesting that the two genes arise from gene duplication. The three ENaC genes α, β, and γ share a remarkable degree of conservation in their genomic organization (45, 169, 213, 249). The human ENaC genes are divided into 13 exons; the 2 transmembrane regions of ENaC proteins are encoded by parts of exon 2 and exon 13. The δ-ENaC gene is located on the chromosome 1.

The promoters of ENaC genes remain to be precisely identified. In human and rat, the region within -75 bp upstream of the transcription start site of the γ-ENaC gene contains two GC-rich boxes that are sufficient for promoter activity (248). Analysis of the nucleotide sequence in the region farther upstream between -289 and -142 shows two imperfect glucocorticoid response elements (GRE) that represent potential transcriptional regulatory elements necessary for ENaC regulation by glucocorticoids (214). Sequential deletions in this region showed that the downstream GRE is sufficient to confer glucocorticoid stimulation and is also able to bind glucocorticoids specifically. An additional third GRE motif further upstream (between -300 and $-2{,}400$) has been identified in the 5′-flanking region of human α-ENaC. Reporter constructs containing this GRE motif also exhibit glucocorticoid-inducible expression (45). So far no specific mineralocorticoid response element has been identified, and the elements that determine the tissue specificity of the glucocorticoid versus mineralocorticoid regulation of ENaC genes remain to be elucidated.

ASIC1, ASIC2, ASIC3, and ASIC4 are located on human chromosomes 12, 17, 7, and 2, respectively (61, 256).

V. ION CONDUCTANCE AND THE CHANNEL PORE

A. Functional Characteristics

The functional properties of the ENaC/DEG channels have been investigated in native tissues and in cell expression systems using electrophysiological techniques. Long before its cloning by functional expression, the highly selective amiloride-sensitive ENaC was functionally characterized in tight epithelia such as frog skin and toad urinary bladder. More recently, ENaC function at the single-channel level could be resolved in the rat cortical collecting tubule using the patch-clamp technique (87). Some members of the ENaC/DEG family exhibit macroscopic ionic currents when expressed in *Xenopus* oocytes, but the single-channel characteristics have not yet been determined (Table 1). Electrophysiological investigations of native *C. elegans* cells are possible but remain difficult because of their small size (91, 165). In cell expression systems, hINaC, BLINaC, and UNC-105 channels simply do not express ionic currents unless an activating mutation is introduced in their sequence. Thus much more functional data on ion permeation are avail-

able for the amiloride-sensitive ENaC channel compared with other family members.

1. ENaC

The macroscopic amiloride-sensitive conductance measured in toad bladder or frog skin was found to be selective for the small inorganic Na^+ and Li^+. In these tissues, the Na^+/K^+ selectivity ratio was estimated to be >500 (20, 185). This high selectivity of ENaC was confirmed at the single-channel level in the mammalian CCD (190) and later in oocytes expressing the α-, β-, and γ-ENaC subunits (138). In the toad bladder an amiloride-sensitive current carried by protons could be measured when the mucosal milieu was acidified below pH 5, indicating that protons can permeate the epithelial Na^+ channel (185, 186). The proton permeability of ENaC expressed in *Xenopus* oocytes has not been addressed yet. Thus ENaC seems to discriminate among cations based on their size, small cations such as Na^+, Li^+, or protons being permeant whereas larger cations such as K^+ or organic NH_4^+ cannot pass through the channel. This simple rule for the ionic permeability of ENaC applies only to monovalent cations, because ENaC is not permeable to divalent cations. In the CCD and in *Xenopus* oocytes expressing α-, β-, and γ-ENaC, the unitary conductance of the amiloride-sensitive epithelial Na^+ channel measured in the presence of 140 mM Na^+ at room temperature is 5 pS (33, 138, 190). A typical trace of ENaC single-channel activity is shown in Figure 5*A*. The single-channel conductance of ENaC saturates at external Na^+ concentrations above 100 mM with a concentration for half-maximal conductance (K_m) around 20–50 mM extracellular Na^+ (138, 184, 192). In the presence of 100–150 mM external Li^+, the single-channel conductance measured at room temperature is 9–10 pS in the cortical collecting tubule and in *Xenopus* oocytes expressing α-, β-, and γ-ENaC. Similar values were measured in a canine kidney cell line (Madin-Darby canine kidney cells) stably transfected with α-, β-, and γ-ENaC (117). The apparent affinity for Li^+ is lower than that for Na^+, with a K_m for Li^+ around 90 mM in cortical collecting tubule and 120 mM in *Xenopus* oocytes (138, 192). A higher dissociation rate of Li^+ from its binding site in the channel pore toward the cytoplasmic side can account for the lower affinity for Li^+ compared with Na^+ and for the faster movement of Li^+ through the channel, i.e., the higher channel conductance for Li^+. These data obtained in the native tissue and in heterologous expression systems set unambiguously the functional conductance signature of ENaC: 4–5 pS and 9–10 pS conductance with Na^+ and Li^+ at concentrations on the order of 100–150 mM and a high Na^+/K^+ selectivity.

The single-channel conductance slightly differs according to the subunit composition of ENaC. In oocytes expressing $\alpha\beta$- or $\alpha\gamma$-ENaC, single-channel conductance is 4–5 pS at 150 mM Na^+. The Li^+ conductance in the presence of 150 mM Li is 9–10 pS in $\alpha\gamma$-ENaC (thus similar to $\alpha\beta\gamma$-ENaC) but similar to the Na^+ conductance in $\alpha\beta$-ENaC (177). The physiological relevance of dimeric $\alpha\beta$- or $\alpha\gamma$-ENaC in native tissues remains uncertain. Several other amiloride-sensitive channels have been described in kidney epithelia (for review, see Ref. 87) which significantly differ from ENaC regarding their biophysical properties. In general, these channels are characterized by a higher conductance in the presence of Na^+, a lower Na^+ over K^+ selectivity ratio, and a lower affinity for amiloride. None of these channels has yet been cloned, and therefore, the relationship between these nonselective epithelial Na^+ channels and ENaC remains to be established.

A controversial issue concerns the relationship between epithelial Na^+ channels reconstituted in lipid bilay-

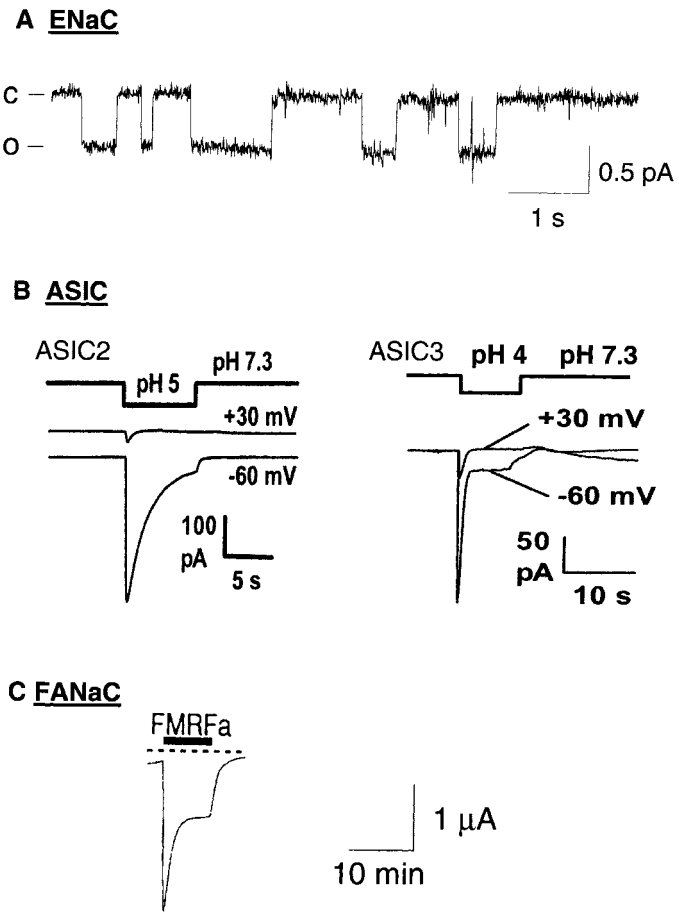

FIG. 5. Functional fingerprints of some ENaC/DEG proteins. *A*: ENaC single-channel trace from an outside-out patch of an oocyte expressing rat $\alpha\beta\gamma$-ENaC in 120 mM Na^+ extracellular solution at −100 mV. C, closed; O, open channel. *B*: H^+-induced currents at two different voltages from COS cells expressing ASIC2 (*left*) or ASIC3 (*right*). [Adapted from Lingueglia et al. (158).] *C*: trace of a current induced by continuous application of 30 μM FMRFamide to an oocyte expressing FaNaC. [Adapted from Lingueglia et al. (157).] Note the difference in time scale between *B* and *C*.

ers and ENaC. Amiloride-sensitive Na^+ channels have been incorporated in lipid bilayers after immunopurification from renal bovine papilla, after in vitro translation of ENaC subunits, or from membrane vesicles of ENaC-expressing *Xenopus* oocytes (121). The unitary currents of these reconstituted channels showed a 40-pS conductance in the presence of 100 mM Na^+ and a low selectivity for Na^+ over K^+ (11, 21, 24, 28, 81, 118–123). To account for this difference, it has been proposed that the lipid environment of ENaC in artificial bilayers, in particular the absence of interactions with the cytoskeleton, could modify the biophysical properties of ENaC reconstituted in lipid bilayers (24, 124, 130, 274). However, recently it has been shown that ENaC reconstituted in planar lipid bilayers retains its functional characteristics: a 6-pS single-channel Na^+ conductance, a slow gating, and a high sensitivity to amiloride (202). Thus it becomes likely that the large-conductance (40 pS) cation channel reconstituted in lipid bilayers by Benos and co-workers (11, 21, 24, 28, 81, 118-123) is not ENaC, and the interpretation of the data obtained from these lipid bilayer reconstitution experiments does not apply to ENaC.

2. ASICs

ASICs are activated by H^+ and inactivate rapidly after activation. Typical ASIC current traces are shown in Figure 5*B*. This transient current carried by Li^+ and Na^+ displays a Na^+/K^+ selectivity ratio $\leq$10. The ASIC single-channel conductance has been determined for several homomeric and heteromeric ASIC channels and ranges from 10 to 15 pS (see Table 1). In contrast to ENaC, ASICs show some permeability to Ca^{2+}. The relative Ca^{2+} permeability is highest in ASIC1a, for which P_{Na}/P_{Ca} permeability ratios of 2.5 (264) and ~17 (18, 240) have been determined. The P_{Na}/P_{Ca} ratio for ASIC3 and ASIC1b is >100 (18, 240). The Ca^{2+} permeability of ASICs remains quite difficult to determine precisely because Ca^{2+} can either block or potentiate ASIC currents depending on its extracellular concentration and the external pH (18, 40, 60, 240). It is possible that the Ca^{2+} permeability of certain ASIC channels might be important for their cellular function.

3. Other channels

UNC-105 is the first degenerin that has been functionally expressed in a heterologous cell system (84). UNC-105 expressed in *Xenopus* oocytes is not spontaneously active, but channel activity could be obtained after introduction of activating mutations (mutations P134S or A692V) that cause muscle hypercontraction and degeneration in *C. elegans* (163, 194). The UNC-105 A692V mutant appears to be nonselective for monovalent cations but shows a selectivity for monovalent over divalent cations with a Na^+/Ca^{2+} current ratio of 20 (84). In *Xenopus* oocytes expressing either one of the two different UNC-105 mutants (P134S or A692V), a channel with a unitary conductance of 4.6 pS for Na^+, thus similar to ENaC, was detected (Table 1). However, conductances ranging from 2–30 pS were also recorded that were attributed to the activity of UNC-105 (84). The MEC-4/MEC-10 channel is selective for Na^+, but no information is available yet on its single-channel properties.

A current trace of the FMRF-gated channel *Ha*FaNaC is shown in Figure 5*C*. *Ha*FaNaC has a low Na^+/K^+ selectivity with a Na^+/K^+ permeability ratio $\leq$10 (157, 272). As for other neurotransmitter-gated channels such as the nicotinic acetylcholine receptor, FaNaC does not need a high cation selectivity to generate an electrical signal in response to the release of neurotransmitters. The unitary conductance of *Ha*- and *Ht*FaNaC with Na^+ as charge carrier is of the order of 7–13 pS (Table 1) (127, 157, 272).

B. Structure-Function Relationship: The Ion Permeation Pathway

According to the way ENaC discriminates among cations, its selectivity filter likely constitutes the narrowest part of the pore, allowing only small cations to pass through the channel (187). Recent mutagenesis studies support the notion that the selectivity filter of ENaC involves a stretch of three conserved amino acids, G/SxS preceding the putative M2 segment in α-, β-, and γ-subunits (135, 137, 138, 223, 231) (Fig. 6). Mutations of residue αS589 in this G/SxS sequence allow larger ions such as K^+, Rb^+, Cs^+, NH_4^+, and divalent cations to pass through the channel consistent with an enlargement of the pore at the selectivity filter (135, 138). Surprisingly, it was found in these mutants that the larger the substituting amino acid was at position α589, the higher was the channel permeability to larger cations. This finding suggests that the side chain of the residue αS589 points away from the pore lumen, which is likely lined by the main chain of the amino acid residues G/SxS (135). An additional argument for such an orientation of the amino acid lining the selectivity filter is the high NH_4^+ permeability in αS589 mutants compared with the smaller cation K^+. The high NH_4^+ permeability is best explained by the formation of hydrogen bonds between NH_4^+ and the carbonyl oxygens of the peptide backbone lining the pore lumen (107, 135). Such a picture of the ENaC narrow selectivity filter lined by the carbonyl oxygens of three amphiphilic residues resembles the basic structure of the K^+ channel selectivity filter, suggesting that similar mechanisms are involved in accommodating the permeant cation.

As predicted by a channel pore surrounded by the three homologous ENaC subunits, mutations in the G/SxS selectivity filter sequence in the β- and the γ-ENaC subunit also reduce the Na^+/K^+ selectivity (138, 223, 231).

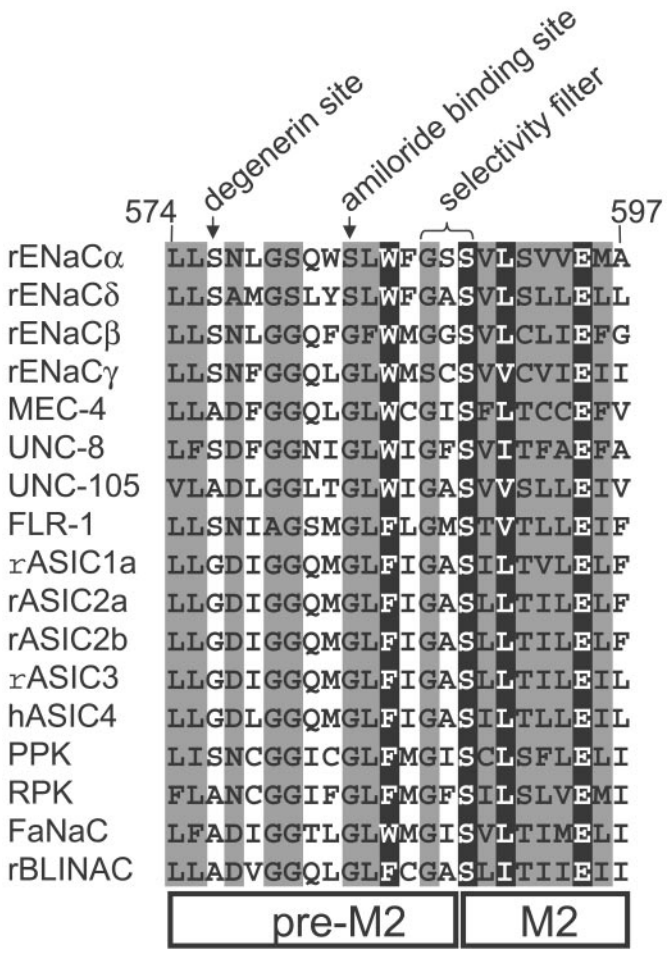

FIG. 6. Alignment of the pore region. The pre-M2 and the NH_2-terminal part of M2 are shown, which make up the outer pore entry and the selectivity filter in ENaC. The location of the degeneration-inducing mutation, the amiloride-binding site, and the selectivity filter are indicated on *top*. Numbering indicates the rat α-ENaC amino acid position. The shading of the residues in the sequence alignment emphasizes the degree of conservation in each column in the alignment. Black shading indicates 100% conserved, and gray shading indicates 80% or greater conserved. Conservative substitutions [based on the similarity group list of equivalent residues in the multiple sequence alignment editor "genedoc" (http://www.psc.edu/biomed/genedoc)] are considered conserved.

The role of the residues homologous to αS589 for the ionic selectivity of other ENaC/DEG channels has not yet been carefully addressed, but the findings that mutations of these residues disrupt function of DEG-1 (85), MEC-4 (108), and ASIC2a (266) point to their critical roles in channel function.

The contribution of residues other than the conserved G/SxS sequence in the channel ionic selectivity remains to be precisely determined. A mutation of a conserved acidic residue (αD602) in M2 to Cys, Ala, or the basic Lys led to a slight increase in the permeability to K^+ (222). The truncation of the cytoplasmic COOH terminus of α-ENaC or mutations of basic residues at the start of the intracellular COOH terminus end have been claimed to increase channel permeability to K^+ (128, 130), but this remains controversial (135). If real, the changes in ENaC selectivity induced by these mutations in the M2 and cytoplasmic COOH terminus remain quite small compared with the changes obtained with mutations of the αS589 and homologous residues (135, 137, 223, 231).

Finally, slight differences have been measured in the Na^+/K^+ permeability ratio for different ASIC channels (Table 1). The generation of ASIC2a-ASIC2b chimeras and subsequent site-directed mutagenesis identified residues of the region preceding the first transmembrane segment that when mutated affect Na^+/K^+ selectivity (Fig. 7) (49). Recently, an ASIC1a/1b chimera approach provided evidence that this region may play a role in the selectivity toward divalent cations (18).

The crystal structure of the KcsA showed that the narrow channel selectivity filter is the site for intimate interactions between the permeating ion and the residues lining the channel pore. In K^+ channels, the oxygens of the carbonyl groups of the polypeptide backbone at the selectivity filter act as surrogate water molecules for the dehydrated ion in the pore (64, 178, 273). The interaction between the ion and these pore residues is essential for ion dehydration and critically depends on the distances

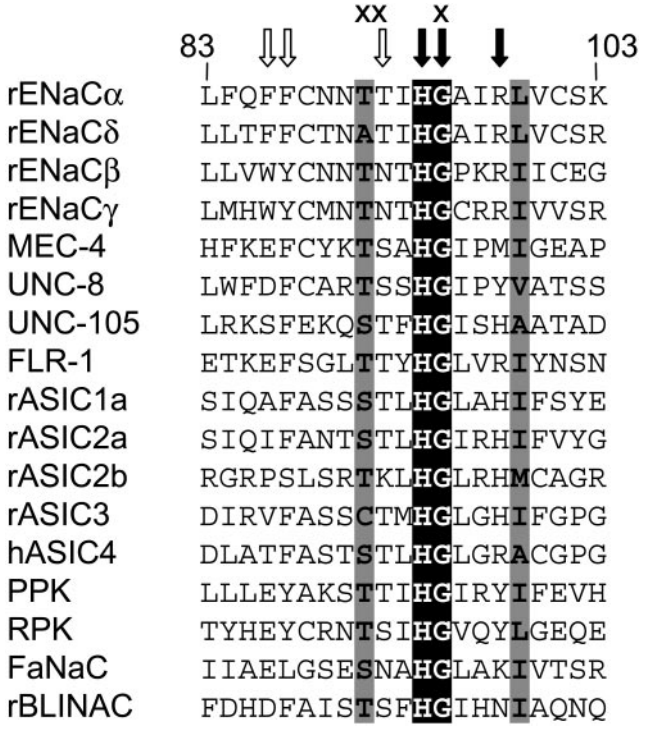

FIG. 7. Alignment of the conserved region in the cytoplasmic NH_2 terminus. Open arrows indicate residues important for ionic selectivity in ASICs (49), black arrows indicate residues important for gating in ENaC (96, 98), and residues marked by a cross are important for MEC-4 function (109). Numbering indicates the rat α-ENaC amino acid position. The shading of the residues in the sequence alignment emphasizes the degree of conservation, as detailed in the legend to Fig. 6.

between the permeating ion and the oxygen atoms. Similarly, changes in the ENaC pore geometry by mutations at position αS589 are expected to perturb these interactions between Na^+ or Li^+ and the pore with functional consequences on the ion conduction. Indeed, the αS589 mutations that cause the highest increase in channel permeability to large cations decrease at the same time the Na^+ and Li^+ single-channel conductance making the channel pore less hospitable for these smaller ions (135, 137). Other mutations within the G/SxS selectivity filter decreased ion conductance. The mutations αG587S, βG529S, and αS589D (Figs. 6 and 8*B*) decreased both Na^+ and Li^+ conductance, mutations γS541A and βG529A decreased selectively the channel conductance for Li^+, whereas the αS588I mutation increased the single-channel conductance for Na^+ (138). These alterations in single-channel conductance were associated with changes in channel affinity for the permeant ion (138). For instance, the low permeability of the γS541A ENaC mutant to Li^+ is associated with a greater than fourfold increase in the channel affinity for Li^+ essentially due to a lower rate of dissociation from its binding site. In this mutant, Li^+ appear to stick to the pore, blocking the Na^+ current if both Na^+ and Li^+ are present (138). The effects of the mutations in the conserved G/SxS sequence on channel conductance and ionic selectivity indicate that this region of the channel pore is essential for the ion recognition and for its permeation through the channel.

Other residues located outside the selectivity filter, αW582, as well as the residues βG525 and γG537 that form the amiloride binding site have been reported to change channel conductance for Na^+ and Li^+ (220, 223). These observations are consistent with close interactions between the amino acid residues lining the outer channel pore and the permeant Na^+ or Li^+. These interactions near the amiloride binding site might be involved in ion dehydration before entering the narrow selectivity filter.

C. Pore Blockers and Putative Binding Sites

1. Pore blockers

Amiloride is a widely used K^+-sparing diuretic that was identified during an extensive screening of some 25,000 compounds susceptible to enhance renal Na^+ excretion and diminish K^+ excretion. Amiloride was found to block the electrogenic Na^+ transport stimulated by aldosterone in the distal nephron by decreasing the apical Na^+ conductance in tight epithelia. The resolution of the apical Na^+ currents at the single-channel level in cortical collecting duct cells directly demonstrated the inhibitory effect of amiloride on ENaC activity by a substantial reduction of the mean open time without changes in the single-channel conductance (104, 190).

Amiloride block has been extensively analyzed in the native epithelial Na^+ channel (reviewed in Refs. 87, 143). ENaC is blocked by submicromolar concentrations of amiloride. Amiloride is a weak base, and the pH dependence of the channel block suggested that the ionized form of amiloride is effective in blocking the channel (see

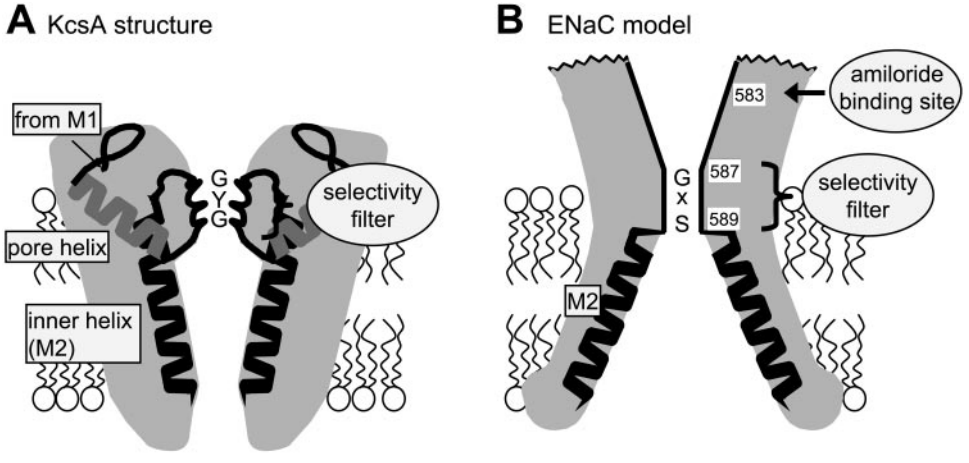

FIG. 8. Model of the pore region of the KcsA K^+ channel and of ENaC. *A*: the model is based on the crystal structure of the KcsA K^+ channel and shows the pore region (64). Two of the four subunits are shown. The second transmembrane domains, the "inner helices," are shown in black; the pore helices are in gray; and the selectivity filter GYG is indicated. *B*: the model of the ENaC pore is based on functional data of wild-type and mutant ENaC. The pre-M2 segments and the second putative transmembrane α-helices (M2) of two of the four ENaC subunits are shown. Amino acid numbering of the α-subunit is indicated. In contrast to KcsA subunits which contain only ~30 residues between the two transmembrane segments M1 and M2, the extracellular portion of ENaC subunits represents >50% of the subunit mass and extends much farther outward than shown in the figure. The outer vestibule is lined by the pre-M2 segments with the site where amiloride binds to αS583 and the corresponding *Gly* residues in β and γ (220). The vestibule narrows down to the selectivity filter formed by αG587, βG529, γS541, and the ring of Ser residues (αS589 and homologous residues in β and γ) (137, 138, 223, 231). In this model the M2 domain forms the intracellular part of the pore, in analogy to K^+ channels.

references in Ref. 87). Consistent with this notion, ENaC block by amiloride depends on the transmembrane potential difference in such a way that hyperpolarization of the membrane increases channel block (see references in Ref. 87 and see Ref. 177). This voltage dependence of channel block is usually interpreted as the effect of the transmembrane potential on the blocker that pulls the charged molecule, i.e., the cationic form of amiloride, toward its binding site located within the transmembrane electric field. This voltage dependence of channel inhibition is typically observed for pore blockers that act by a simple physical occlusion of the pore. Quantitative analysis indicates that the charged guanidinium moiety experiences 15–30% of the transmembrane electrical field when the molecule is bound to its blocking site. As expected for a pore blocker, amiloride interacts with permeating Na^+ and Li^+. Raising the extracellular concentration of Na^+ reduces the channel affinity for amiloride. Experiments in the toad bladder convincingly showed that the interaction between the permeant Na^+ and amiloride was competitive, suggesting overlapping binding sites within the external ion permeation pathway (189). In other epithelia, experiments addressing this issue did not allow a clear demonstration of a strict competitive interaction between the permeating Na^+ and amiloride (reviewed in Ref. 87).

Both the charged guanidinium group and the pyrazine ring of amiloride are necessary for high-affinity binding. Guanidinium itself and pyrazine analogs such as 6-chloro-3,5-diaminopyrazine-2-carboxamide (CDPC) can block the channel, with apparent affinities of ~100 mM for guanidinium and 100 μM for CDPC. Addition of a benzyl or a phenyl group to the guanidinium side chain of amiloride (e.g., benzamil or phenamil) increases the affinity of block by a factor of ~10 for the epithelial Na^+ channel (143). This suggests that hydrophobic interactions with a part of the channel or the membrane very close to the amiloride binding site can stabilize the bound state of the drug.

A variety of organic and inorganic cations block ENaC with low affinity from the extracellular side in a voltage-dependent manner (187). Their ability to block ENaC critically depends on their size, namely, a molecular diameter lower than 5 Å. The voltage dependence of the block by inorganic cations is steeper than the block by amiloride or other organic cations, suggesting that the smaller inorganic cations penetrate deeper into the channel pore. From the analysis of the external channel block by cations it was proposed that the pore progressively narrows down to a binding site that accepts smaller inorganic cations and finally to the narrowest part of the pore, the selectivity filter, that accommodates exclusively the permeating ions H^+, Li^+, and Na^+ (187).

All ENaC/DEG channels other than ENaC require about 100-fold higher amiloride concentrations for channel block, except for Mec-4/MEC-10 channels whose sensitivity to amiloride block is between that of ENaC and that of other ENaC/DEG family members (Table 1). It is not clear whether the mechanism of channel block by amiloride is common to all ENaC/DEG channels. It should be remembered that at concentrations in the higher micromolar range amiloride blocks many other ion channels and transporters that are unrelated to ENaC, likely by different molecular mechanisms (143).

No specific pharmacological blockers of ASICs are available so far except for a toxin from tarantula venom that has been found to specifically block homomultimeric ASIC1a with high affinity (IC_{50} = 0.9 nM) (72). Psalmotoxin 1 (PcTX1) is a 40-amino acid toxin from the venom of the South American tarantula *Psalmopoeus cambridgei*. PcTX1 has a limited overall homology to other spider venom toxins identified to date. PcTX1 blocks rapidly and reversibly recombinant homomeric ASIC1a only, but not the homomultimers ASIC1b, ASIC2a, ASIC3a, or the heteromers ASIC1a/ASIC2a or ASIC1a/ASIC3a, nor $\alpha\beta\gamma$-ENaC or K^+ channels.

ASIC currents are inhibited by divalent and trivalent cations. Ca^{2+} inhibit Na^+ currents in several different ASIC multimers with an apparent IC_{50} in the millimolar range (38, 40, 60, 240, 264). As mentioned earlier, the interactions of ASICs with Ca^{2+} that can also permeate ASICs are complex and not completely understood. Recently, it was shown that lactic acid, which is produced by anaerobic metabolism during ischemia, enhances ASIC function by chelating divalent cations that in the absence of lactate partially inhibit ASIC function (113). This mechanism may be of physiological importance making ASICs extra sensitive to lactic acidosis of local ischemia.

In mutant UNC-105(A692V) channels, Na^+ currents are blocked by Ca^{2+} and Mg^{2+} with an IC_{50} of 25 mM. Gd^{3+} is a blocker of mechanosensitive channels with an IC_{50} of the order of 10–100 μM (103). Currents through RPK/dGNaC1 channels are blocked by Gd^{3+} with an IC_{50} of 100 μM (3). ASIC3 homomultimers and ASIC2a/ASIC3 heteromers are also sensitive to Gd^{3+} with an IC_{50} ~40 μM compared with >1 mM for ASIC2a homomeric channels (12). The sensitivity of ASICs and RPK channels to Gd^{3+} does by no means indicate that these channels are mechanosensitive.

2. The amiloride binding site

A mutagenesis screen of the amino acid residues preceding the M2 transmembrane segment of α-, β-, and γ-ENaC identified residues in the β (βG525) and at the homologous position of γ-ENaC (γG537), each of which when mutated reduces the apparent channel affinity to amiloride by ~1,000-fold (see Figs. 6 and 8*B*) (220). The homologous αS583C mutation reduces the affinity to amiloride by ~20-fold. Because amiloride acts as a pore

blocker, these observations demonstrated for the first time that the pre-M2 segments of ENaC subunits form the outer pore and that all three subunits line the ENaC pore like barrel staves (188). Introduction of Cys residues at position S583 of α-ENaC generates a high-affinity binding site for zinc ions that also block the channel in a way very similar to amiloride (220). According to the α-β-α-γ subunit arrangement around the channel pore in which the two α-subunits face each other (76, Fig. 4*A*) and given the optimal distance of two sulfhydryl groups for coordinated ligation of Zn^{2+} (149), the diameter of the pore at position αS583 can be estimated to be ~5 Å. Amiloride, which has a diameter of 4–5 Å, would fit snugly into the outer channel pore.

The 1,000-fold change in channel affinity for amiloride caused by the mutations βG525 or γG537 suggests that these residues are directly involved in binding interactions with amiloride. The observation that sulfhydryl reagents such as MTSEA or Zn^{2+} are able to reproduce channel block when binding to Cys residues introduced in the amiloride binding site at corresponding αS583, βG525, or γG537 positions in the ENaC subunits strongly supports that these residues are part of a blocking site in the channel pore with affinity for amiloride (146, 220, 229). The ENaC/DEG channels exhibit a wide range of affinities for amiloride (Table 1), and comparison of their primary sequences indicate that the Gly residues β525 and γ537 that are crucial for the high affinity of ENaC for amiloride are completely conserved except for the α- and δ-ENaC subunits which contain at the corresponding position a Ser (αS583). The δ-ENaC subunit can substitute the α-subunit to make functional channels (265). This combination of the Ser residue on α (αS583) and the Gly residues on β and γ (β525 and γ537) within the amiloride binding site likely represents the structural basis for the unique high affinity of ENaC for amiloride block. Consistent with this hypothesis it was found that mutation of αS583 to Gly results in a ~20-fold decrease of the apparent amiloride affinity (S. Kellenberger, I. Gautschi, and L. Schild, unpublished data).

The short amino acid segment WYRFHY NH_2-terminal of CRDII in the α-ENaC extracellular loop was proposed to participate in amiloride binding interactions with ENaC and therefore with channel block. This putative amiloride binding site was identified based on sequence homology with an antibody that recognizes limited regions of amiloride. The homology between ENaC and the antibody is rather low within the WYRFHY segment and involves only the two Tyr and the His residues (125, 141). The WYRFHY deletion mutant (αΔ278–283) coexpressed in *Xenopus* oocytes with wild-type β- and γ-ENaC subunits did not express enough current to determine the apparent amiloride affinity (125, 138). A His to Asp substitution within the WYRFHY sequence was found to decrease amiloride affinity in ENaC reconstituted in lipid bilayers (125), but the mutant channel coexpressing αH282D with wild-type β- and γ-ENaC in *Xenopus* oocytes has the same affinity for amiloride as ENaC wild-type (138). Thus the αWYRFHY sequence in the context of αβγ-ENaC does not represent an amiloride binding site involved in channel block. It should be mentioned that in all other cases of amino acid substitutions reported to cause channel resistance to amiloride that were based on experiments in lipid bilayers, not a single one was confirmed on ENaC expressed in *Xenopus* oocytes (81, 121, 125). Thus the available experimental data indicate that amiloride occludes the external channel pore by binding to a high-affinity site constituted by αS583 and the conserved *Gly* residues of β- and γ-ENaC subunits (βG525, γG537) located in the pore domain preceding the putative M2 segment (Fig. 8*B*).

In two of the cloned FaNaC orthologs amiloride has opposite effects. While it blocks *Ha*FaNaC (of *Helix aspersa*), it potentiates FMRFamide responses in *Ht*FaNaC (of *Hexisoma trivolvis*). With the use of a chimeric approach, a region of ~120 amino acids in the NH_2-terminal part of the extracellular loop was identified which determines whether amiloride acts as agonist or antagonist on FaNaC channels (52). This region is also critical for the concentration dependence of the channel activation by FMRFamide. It is interesting to note in this context that the guanidinium compound benzimidazolyl-guanidine (BIG) can potentiate ENaC in the frog skin by abolishing the channel self-inhibition by external ions (271).

PcTX1 specifically inhibits ASIC1a channels, but the mechanism of channel inhibition remains unclear. The splice variant ASIC1b is not sensitive to PcTX1 block (72) and differs from the ASIC1a essentially in the intracellular NH_2 terminus, the transmembrane segment M1, and the first 110 residues of the extracellular loop. Considering that the toxin acts from the extracellular side it was proposed that the PcTX1 binding site in ASIC1a is located in the NH_2-terminal 110 amino acids of the extracellular loop.

D. A Model of the Channel Pore

The only available high-resolution structure of a highly selective cation channel is that of the KcsA K^+ channel. Certain comparisons with the possible structure of ENaC can be made, although there is no homology between the two proteins. A schematic view of the KcsA pore region is shown in Figure 8*A*. As ENaC, KcsA contains two transmembrane regions. These are linked on their extracellular ends by the ~30 amino acids forming the pore region, whereas the NH_2 and COOH termini are intracellular. The KcsA is a tetramer, like all other known K^+ channels, and the subunits are related by a fourfold axis of molecular symmetry around the central ion-con-

ducting pore. The architecture of the channel pore is primarily defined by four inner helices formed by the second transmembrane region M2 (black helices in Fig. 8*A*). The inner helices are tilted with respect to the membrane normal by ~25° and are slightly kinked so that the subunits open like the petals of a flower facing the outside of the cell. The open petals house the structure formed by the pore region near the extracellular surface of the membrane. The narrow selectivity filter that is located in this region is only 12 Å long, whereas the remainder of the pore is wider and lined with hydrophobic amino acids of M2. The pore entrance and selectivity filter are formed by the ~30 amino acids between the two transmembrane regions. For each subunit, in going from the NH_2 to the COOH terminus, this comprises a small extracellular structure called the "turret" and the pore helix (gray in Fig. 8*A*) which slots between the inner helices and points to the intracellular end of the selectivity filter. The pore helix is followed by the selectivity filter GYG that is separated from M2 by a linker of approximately seven residues. K^+ permeation is thought to depend critically on a tight match between the size of the ion and the geometry of the pore at the selectivity filter.

Comparison of ENaC with KcsA is presently limited to the outer pore region, since the structures that constitute the internal pore beyond the selectivity filter have not been clearly identified so far in ENaC. Similarities between ENaC and the KcsA channel include the location of the narrow selectivity filter toward the extracellular solution, the narrow selectivity filter consisting of three conserved residues in each subunit, and the apparent orientation of the side chains of these residues away from the pore lumen. However, clear differences exist between ENaC and KcsA in particular regarding the topology of M2 relative to the selectivity filter and the external binding sites for blockers. In KcsA the sequence preceding the GYG selectivity filter dips into the membrane, and the GYG sequence is oriented with the COOH-terminal end toward the extracellular side, then a seven-amino acid linker separates the selectivity filter from the M2 transmembrane segment helix (Figs. 6 and 8) (64). In ENaC there is no linker between the selectivity filter sequence αG587-S589 and the start of M2 segment (138, 223). The sequence preceding the ENaC selectivity filter is the site for binding of large blocking molecules such as amiloride that enter the pore from the extracellular solution. A model based on the KcsA channel structure would locate the amiloride binding site deep into the channel pore beyond the narrow selectivity filter. More likely, the ENaC pre-M2 segment extends from the NH_2 terminus of M2 toward the extracellular side, which is supported by the observation that a Cys introduced at position G536 in human γ-ENaC within the amiloride binding site (corresponding to αS583) is accessible to the hydrophilic sulfhydryl reagent MTSET from the extracellular side (231). Thus the six amino acid residues of the pre-M2 and the very first residue of the putative M2 segment (Figs. 6 and 8*B*) likely represent the outer ENaC pore that narrows from the amiloride binding site down to the ion selectivity filter.

Within families of ion channels such as the voltage-gated or the ligand-gated ion channels, there is a remarkable homology in the structure of the ion permeation pathway (160). Furthermore, within the large family of K^+ channels, the pore structure is not only conserved, but basic physicochemical principles of K^+ permeation are also similar. So far, the pore of ENaC has been the best characterized among the members of the ENaC/DEG channel family, and it is likely that the basic structural features of the channel pore are conserved within this family. However, a possible involvement of a region in the pre-M1 domain in ion selectivity has been described in ASICs but not ENaC (18, 49, 98) (see sect. v*B*). In addition, involvement of the M1 segment of FaNaC was proposed in a recent study that applied the substituted cysteine accessibility method (SCAM) (197). Cysteine residues introduced at seven different positions in M1 were accessible to modification by externally applied sulfhydryl reagents that inhibited 50–60% of the FaNaC current. Inhibition was prevented if the sulfhydryl reagents were applied in the presence of amiloride. These findings were interpreted as the demonstration that M1 of FaNaC lines the channel pore. However, channel inhibition by hydrophilic sulfhydryl reagents can occur by different mechanisms, as, e.g., effects on gating or on ion permeation. Thus the present evidence for a M1 segment lining the external channel pore remains quite weak, and more detailed functional and structural studies are necessary to draw a clearer picture of the role of the intracellular NH_2 terminus in ASICs and the M1 in FaNaC in ion conduction.

VI. CHANNEL GATING

A. Channel Activation

Channel gating is probably the most variable function among the members of the ENaC/DEG family: some channels open in response to mechanical stimuli, others in response to external ligands, and some are constitutively active. Mutations in both intracellular and extracellular domains affect channel gating.

1. ENaC

ENaC is constitutively active in the apical membrane of tight epithelia. Single ENaC recordings in the cortical collecting tubule show slow kinetics with open and closed dwell times in the range of seconds at room temperature (190). Similar gating properties are observed in

oocytes expressing $\alpha\beta\gamma$-ENaC shown in Figure 3*A*. The systematic analysis of ENaC single-channel gating kinetics reveals that the open probability (P_o) of the channel varies from <0.1 to 0.9 and that active ENaC channels can be divided basically into two groups: one with a low P_o and long closed times and the second with high P_o and long open times. These variations in the ENaC P_o likely reflect different channel gating modes (193). Presently it is not clear how these gating modes are influenced by extracellular and intracellular factors. For instance, external Na^+ decreases channel activity by a mechanism termed "self-inhibition." The physiological role of this Na^+-induced channel inhibition is not clear, but it could play a role in maintaining a homogeneous Na^+ reabsorption along the nephron (87, 184). Intracellular pH, Ca^{2+} (35, 191), or Na^+ exert a feedback inhibition on the channel (1, 62, 80, 136, 191, 227). Finally, enzymes such as serine proteases or channel activating protein (CAP)-1 that are expressed in tight epithelia stimulate channel activity when coexpressed with ENaC in *Xenopus* oocytes (254, 262). This activation of ENaC is also observed in *Xenopus* oocytes after addition of a low concentration (2 μg/ml) of trypsin to the extracellular side (46). The physiological relevance of the serine proteases in ENaC regulation is still unknown.

2. ASICs

In general, ASICs display a transient peak current activated by protons that lasts hundreds of milliseconds to seconds, followed by a channel desensitization despite the continued presence of a low external pH solution (Fig. 5*B*). The pH of half-maximal activation of ASIC currents depends on the channel type. Transient currents carried by homomeric channels formed by ASIC1a, -1b, or -3 show pH values of half-maximal activation ($pH_{50\ activation}$) of the range of 5.9–6.5. ASIC2 is less sensitive to pH changes and displays a $pH_{50\ activation}$ of 4.4. It has been shown for ASIC1a (264) and ASIC2a (38) that only extracellular and not intracellular protons activate the channel.

Desensitization varies among the different ASIC channels: for instance, ASIC1 and ASIC3 desensitize faster than ASIC2 (Fig. 5*B*). Under certain conditions, inactivation of the current carried by some ASIC multimers is incomplete, leaving a sustained residual inward current that follows the fast transient current. This sustained current is found during prolonged acidification in cells expressing ASIC3 homomultimers or the heteromers ASIC2a/ASIC2b, ASIC2a/ASIC3, and ASIC2b/ASIC3 (12, 13, 61, 158, 263, 267). Surprisingly, the sustained currents in ASIC-expressing cells exhibit biophysical and pharmacological characteristics different from the transient currents (25, 263). The reasons for these functional differences are not clear. Transient and sustained currents might involve distinct ASIC channel types, or the sustained currents could represent leakage currents due to ASIC overexpression in the cell. Finally, it remains possible that ASICs change their biophysical and pharmacological characteristics during activity as documented for the purinergic P2X7 (239) and for neuronal P2X receptors (140, 258) and for K^+ channels undergoing C-type inactivation (234).

From the rather nonphysiological pH for half-maximal activation of some ASICs, it has been hypothesized that endogenous ligands might shift channel activation toward more physiological pH values. Zn^{2+} at physiological concentrations potentiates the acid activation of homomeric or heteromeric ASIC2a channels by shifting the pH dependence of activation to higher values (16). Although ASICs are not the mammalian homologs of FaNaC, FMRFamide and related neuropeptides have been found to modulate ASIC currents (8). FMRFamide is a neurotransmitter in invertebrates only, but the related neuropeptides FF or AF are expressed in the mammalian CNS (8). Administration of FMRFamide to mammals induces a variety of physiological effects, including alterations in blood pressure, respiratory rate, glucose-stimulated insulin release, pain perception, and behavior, some of which are mediated through opioid receptors (reviewed in Ref. 8). Coapplication of FMRFamide at micromolar concentrations with protons slows inactivation of the proton-induced current and induces a noninactivating inward current. This sustained current at the end of a 30-s application is on the order of 10% of the peak current. A similar although considerably smaller effect could be induced by application of the mammalian peptide neuropeptide FF. This modulation of ASIC activity by neuropeptides might be of physiological relevance in pain sensation (25, 267). Recently, it was shown that FMRFamide or neuropeptide FF potentiate the acid-induced peak current and slow the inactivation of ASIC2A/3 heteromers expressed in *Xenopus* oocytes (34).

3. FaNaC

Extracellular application of the peptide FMRFamide to cells expressing FaNaC induces a fast inward current that displays a slow and partial desensitization in the presence of the agonist (see Fig. 5*C*). The EC_{50} for FMRFamide-induced activation depends on the FaNaC ortholog and is 2–70 μM (157, 272). The agonist specificity for channel activation was recently investigated in *Ha*FaNaC expressed in *Xenopus* oocytes, and several agonists have been identified (51, see Table 1 therein and Ref. 157). HaFaNaC was the first FaNaC to be cloned and is the best studied so far. The single-channel kinetics in the presence of the activating ligands FMRFamide or FLRFamide are complex and involve transitions between several open and closed states. The dwell times are of the order of hundreds of microseconds to several milliseconds (272).

At higher concentrations of the activating peptide the number of long openings increases. Based on this kinetic analysis and a Hill coefficient of activation of >1, it was suggested that *Ha*FaNaC binds two agonist molecules for full activation of the channel (157, 272). At concentrations ≥30 μM, the agonists FMRFamide and FLRFamide block the channel (93).

4. Degenerins

The molecular mechanisms underlying channel opening in response to mechanical stimuli remain poorly understood for the degenerins and likely involve complex interactions between the different proteins that form the mechanotransducing complex (Fig. 4*B*). Mechanosensitivity of UNC-105 alone or MEC-4/MEC-10 together with MEC-2 expressed in heterologous cell systems could not be demonstrated, suggesting that other associated or interacting proteins are necessary for this function. While wild-type MEC-4/MEC-10/MEC-2 expressed in *Xenopus* oocytes displays amiloride-sensitive current, UNC-105 requires activating mutations to induce channel openings (84, 90).

B. Gating Domains

The generation of ENaC/DEG channel mutations of conserved amino acid residues changing the channel openings and closures identified specific regions in the extracellular loop and in the cytoplasmic NH_2 terminus that control channel gating.

1. Extracellular gating domains

The first evidence for the contribution of a site in the extracellular loop to channel gating came from the identification of mutations in the pre-M2 region of the degenerin MEC-4 that cause degeneration of touch receptor neurons in *C. elegans* (Fig. 3*B*). The morphological features of this degenerative phenotype are consistent with an abnormal leak of cations into the neuronal cell due to a serious channel dysfunction consisting presumably in abnormal openings and/or inefficient closures of the touch receptor channel complex. The *mec-4* alleles causing the dominant degenerative phenotype encode substitutions of the conserved residue A713 in the pre-M2 region (Fig. 6) by large side chain amino acids, whereas A713 substitutions by small side chain amino acids (Ala, Ser, Cys) are without effects on the cell (65). It was hypothesized that the presence of a bulky side chain at position A713 within an extracellular gate may prevent the channel from closing efficiently.

Subsequently, it was shown for most ENaC/DEG family members that this conserved residue plays an important role in channel gating. Substitution of the residue homologous to MEC-4 A713 in ASIC2a, G430, by large residues results in constitutively active channels (4, 266). In addition to the constitutive currents in the ASIC2aG430 mutants, H^+-gated currents can still be activated by lowering of the pH (38). The H^+-gated current in G430 mutants differs from the wild-type current in two aspects. Inactivation of the H^+-activated ASIC2a current is slowed in Ser or Cys G430 substitution mutants (which do not display a constitutive current) and is completely disrupted by the larger substitutions Thr and Phe (38). These mutations also shift the pH dependence of activation to less acidic pH values. The size of the pH shift and the degree of disruption of inactivation correlate with the ability of the substitution to induce a constitutive current, indicating that these different aspects of channel function related to H^+ gating are linked. Thus the G430 mutation seems to favor the active conformation of the channel and prevent the channel from relaxing back to an inactivated or resting state. The role of G430 in ASIC2a in gating is further supported by the observation that this residue undergoes conformational changes during channel activation (4, 6). Covalent modification of a *Cys* residue at position G430 in the ASIC2a G430C mutant by hydrophilic MTS sulfhydryl reagents is possible only when the channel is activated by protons. Thus, in the activated state, the C430 is accessible to extracellular MTS reagents leading to a noninactivating current that persists even after switching the pH back to resting pH (4). This G430C mutant can also be activated by Zn^{2+} at pH values at which the channel is normally closed, suggesting that the engineered Cys at the degenerin site may be accessible to small ligands such as Zn^{2+} independently of the conformational state (6). Alternatively, Zn^{2+} which is a known coactivator of ASICs may react with endogenous His residues and induce a conformational change that exposes the Cys to the extracellular solution (16). The mutation of the homologous residue in ASIC2b, G481 to Phe was characterized in ASIC2a/2b heteromers, because ASIC2b does not form functional channels by itself (251). This mutation completely disrupted inactivation but did not change any other functional parameters. Introduction of a cysteine residue at the position corresponding to G430 in α- or β-ENaC subunits and its covalent modification by sulfhydryl reagents induces an increase in the channel P_o (228). As for ASIC, the cysteine modification leading to channel openings is observed when the channel is in the open conformation. Thus the conserved extracellular "degenerin" residue is tightly involved in opening and closing of ENaC/DEG channels.

Another extracellular regulatory domain named "ERD" was found between the cysteine-rich domains CRDI and CRDII in a region unique to the degenerins (85). Activating mutations in the ERD domain were found in DEG-1, MEC-4, and UNC-8. The *mec-4* alleles harboring a missense mutation (A404T) or a small deletion (Δ399–

407) in the ERD induced neuronal degeneration in *C. elegans* (85). Similarly to the degenerin site at the pore entrance, touch cell death also resulted from the substitution of large-side-chain amino acids (Thr, Leu, or Lys) but not small-side-chain amino acids (Gly or Cys) for Ala in MEC-4.

The post-M1 (pM1) domain is highly conserved among all the ENaC/DEG family members (Fig. 3) (84). A mutation that causes muscle hypercontraction consistent with a channel gain-of-function mutation has been identified in this region of the degenerin UNC-105P134S (163). Expression of the UNC-105 P134S mutant in *Xenopus* oocytes confirmed changes in the channel P_o and gating kinetics (84). There is currently no evidence indicating that the post-M1 region also contributes to gating of ASIC or ENaC channels. A loss-of-function mutation causing PHA-I was found in this post-M1 region of α-ENaC. So far, there is no evidence for an effect of this Cys substitution on channel gating (see sect. VII) (77, 95). Finally, inactivating mutations were found in CRDIII and in the pre-M2/M2 domain (85, 108, 109). It is unclear how these mutations can be strictly assigned to defects in channel gating, or whether they impair channel function by affecting the biosynthesis, maturation, or targeting of the channel complex to the cell surface.

Zinc is a coactivator of ASICs. Two His residues have been identified that are essential for the activating effect of Zn^{2+} in ASIC: one in the CRDII and one directly COOH terminal of CRDIII (Fig. 3) (16). In the course of this analysis, a His residue was identified that abolishes the pH sensitivity of ASIC2a when mutated. This residue is located directly COOH terminal of M1 and seems to be an essential component of the extracellular pH sensor.

2. An intracellular gating domain

A loss-of-function mutation in the highly conserved HG motif (Figs. 3 and 7) preceding the first transmembrane segment of β-ENaC was found to be associated with the renal salt-losing syndrome PHA-I (see sect. III*A*) (39). When expressed in *Xenopus* oocytes, the βG37S mutation causing PHA-I as well as mutations of the corresponding Gly residues in α- or γ-ENaC subunits result in an important reduction in channel P_o (39, 96, 98). Surface expression of the channel is not affected by these Gly to Ser mutants. Thus these mutations point to a role of the intracellular pre-M1 segment in channel gating. Mutations of the conserved neighboring residues of the homologous Gly residue in α-ENaC (G95), H94 and R98, resulted in a similar channel inhibition (Fig. 7) (98). It remains to be elucidated how these residues control channel gating. Interactions between subunits, with intracellular proteins or with ligands, and phosphorylation events are possibilities that remain to be experimentally addressed. Biochemical evidence suggests that an NH_2-terminal fragment of the γ-ENaC subunit may interact with the α-subunit and modulate channel activity (5).

Recently it was demonstrated that mutations in the homologous region of MEC-4, T91I, S92F, or G95E (Fig. 7) disrupt touch sensation in *C. elegans* (109). In addition, it was shown that overexpression of a peptide corresponding to the intracellular NH_2 terminus of MEC-4 dramatically increased the fraction of touch-insensitive animals in the wild-type background and that it caused a significant reduction in the number of degenerating touch neurons in transgenic animals expressing the A713V degenerin mutation. This experiment thus suggests that the NH_2 terminus of MEC-4 is involved in protein-protein interactions. If the NH_2-terminal peptide contained either of the mutations T91I, S92F, or G95E, the interference with MEC-4 was almost completely abolished, indicating that this short conserved domain is critical for the interaction (109).

VII. CHANNEL REGULATION

The regulation of channel activity at the cell surface by intracellular messengers or by hormone-induced cascades of cellular events is well established for ENaC, but not for ASICs or other ENaC/DEG family members, and it is unknown whether at all and how the activity at the cell surface of these other ENaC/DEG channels might be regulated.

A. Transcriptional and Posttranscriptional Regulation

The excretion of sodium by the kidney has to balance the daily salt intake. The site of fine regulation in the kidney is the distal nephron where Na^+ absorption from the urine via ENaC is under the control of hormones. In response to a decrease in extracellular fluid volume or to hyponatremia the renin-angiotensin-aldosterone cascade is activated leading to an increase in Na^+ reabsorption in the distal nephron (257). Aldosterone binds to a cytosolic receptor, and this hormone-receptor complex is translocated to the nucleus where transcriptional events occur leading to an increase in ENaC mRNAs and other aldosterone-induced transcripts (AITs) together with a decrease of the level of aldosterone-repressed transcripts (ARTs) (Fig. 2) (167, 168, 172, 174, 206, 237). The AITs and ARTs are key elements for the upregulation of ENaC at the apical membrane and of the Na^+-K^+-ATPase at the basolateral membrane by aldosterone allowing the stimulation of a transepithelial Na^+ flux. Recently, it was shown that aldosterone rapidly increases the mRNA level of the serine/threonine kinase "serum- and glucocorticoid-regulated kinase" (SGK), and it was demonstrated that SGK stimulates ENaC when coexpressed in *Xenopus*

oocytes (42, 59, 180, 195). It has been clearly demonstrated that the early effect of aldosterone consists in a marked redistribution of ENaC from a cytoplasmic pool to the apical membrane (166–168, 172). This increase in ENaC channel density at the cell surface is thought to contribute essentially to the early response to aldosterone which increases Na^+ transport within 1–3 h of stimulation by the hormone.

Vasopressin (AVP) increases both water and Na^+ absorption in the distal nephron (79, 115, 181, 182, 217). Binding of AVP to AVP receptors (V2 receptors) at the basolateral membrane of principal cells causes a redistribution of aquaporins (AQP-2) from an intracellular compartment to the apical membrane leading to an increase in cell membrane water permeability. In parallel, the stimulation of the V2 receptors increases ENaC activity at the apical membrane that accounts for the enhanced Na^+ absorption. Both AVP effects on AQP-2 and ENaC are mediated by cAMP and can be mimicked by cAMP analogs or forskolin (115).

B. Cell Surface Regulation

The specific targets on ENaC for the regulation of channel activity by aldosterone or AVP likely reside in the intracellular NH_2 and/or COOH termini. The COOH termini of $\alpha\beta\gamma$-ENaC subunits have a low homology except for a conserved proline-rich motif that includes three adjacent Pro residues separated by one residue from a downstream Tyr, the PPPxY or "PY" motif. This PY motif is found exclusively on the ENaC subfamily members. This motif on β- and γ-subunits is mutated or deleted in a rare form of monogenic hypertension, Liddle's syndrome (105, 106, 114, 152, 218). Missense or deletion mutations within the PY motif of β- or γ-ENaC result in a retention of hyperactive channels at the cell surface after expression in *Xenopus* oocytes, suggesting that the conserved Pro and Tyr are involved in the internalization of ENaC at the cell surface (78, 136, 226).

The amino acid sequence encompassing the PY motif in α-, β-, and γ-ENaC shows two adjacent endocytic motifs, NPxY and YxxL, that are recognized by the clathrin: Ap-2 complex (226, 232). These endocytic motifs could play a role in removing ENaC from the plasma membrane via clathrin-coated pits. Dynamin is required for clathrin-mediated endocytosis. Expression of catalytically inactive dynamin mutants with ENaC results in an increase in ENaC activity at the cell surface of similar magnitude as that obtained by mutations in the ENaC PY motif (226). Other investigations followed the hypothesis that the PY motif is involved in specific protein-protein interactions involving binding of the cytoplasmic PY motif to conserved Trp-Trp (WW) domains. The WW domains are protein-protein interaction modules that bind to proline-rich sequences. With the use of a yeast two-hybrid screen with a PY motif as bait for a binding partner of ENaC, neuronal precursor developmentally downregulated 4 (Nedd4) was shown to bind to PY motifs of β- and γ-ENaC and with a lower affinity to the PY motif of α-ENaC (235). Recently, the structure of the binding complex between a Nedd4 WW domain and the ENaC PY motif has been solved by NMR spectroscopy (133).

Nedd4 is a ubiquitin protein ligase with conserved WW domains that specifically interact with PY motifs. Ubiquitin ligase is responsible for attachment of ubiquitin chains to Lys residues of the target protein as a tag for rapid protein degradation. Evidence that Nedd4 regulates channel activity comes from functional coexpression of ENaC together with Nedd4 in *Xenopus* oocytes (2). The ENaC-Nedd4 coexpression results in an almost complete inhibition of channel activity at the cell surface due to a corresponding decrease in the number of channel molecules at the plasma membrane of oocytes. Conversely, channel activity was increased and active channels were retained at the cell surface when ENaC was coexpressed with a catalytically inactive Nedd4 mutant. This Nedd4 mutant is still able to bind PY motifs of ENaC but unable to ubiquitinate the channel, and it therefore competes with the endogenous Nedd4 of the *Xenopus* oocyte (2). These findings are consistent with a regulation of ENaC at the cell surface that involves binding of Nedd4 ubiquitin ligase to the PY motifs of β- and γ-ENaC leading to channel ubiquitination, endocytosis, and degradation via the proteasome and/or the endosomal pathway. It should be pointed out that clathrin-mediated endocytosis and ubiquitination are not mutually exclusive mechanisms and could both coregulate ENaC activity at the cell surface.

The specificity of the interaction between the PY motifs in α-, β-, and γ-ENaC subunits and protein partners in different tissues where ENaC is expressed needs further investigation. Different homologs of Nedd4 have been identified with different ability to interact with ENaC and to modulate its activity in *Xenopus* oocytes (132). Finally, the contribution of the PY motifs in the control of ENaC activity at the cell surface by aldosterone or AVP remains to be established. When coexpressed in *Xenopus* oocytes, the aldosterone-induced kinase Sgk can phosphorylate and inactivate Nedd4 leading to a retention of ENaC at the cell surface (58). The relevance of this signaling pathway in aldosterone-responding cells remains to be demonstrated.

Further support for a role of Nedd4 in the regulation of ENaC at the cell surface comes from the fact that ENaC is ubiquitinated in *Xenopus* oocytes. The ubiquitination sites involve the Lys residues in the NH_2 terminus of α- and γ-ENaC. Expression of ubiquitination-deficient ENaC mutants by substitution of Lys to Arg in the NH_2 terminus of α- and γ-ENaC considerably decreased channel ubiq-

uitination and increased the number of active channels at the cell surface (235, 236). Finally, the PY motif on ENaC might be involved in feedback regulation of the channel activity by intracellular Na^+. Wild-type ENaC is downregulated by intracellular Na^+. Liddle mutants have a considerably lower sensitivity to inhibition by intracellular Na^+ at least when expressed in *Xenopus* oocytes (136). How intracellular Na^+ may activate the ENaC-Nedd4 interaction is not known.

Chalfant et al. (36) have systematically approached the functional role of the intracellular NH_2 terminus in ENaC. NH_2-terminal truncation up to residue 46 did not affect currents through ENaC formed by the truncated α- and wild-type β- and γ-subunits. Different truncations of the first 51 up to the first 67 residues increased the current by about fourfold, and truncations of the first 79 or more residues abolished the amiloride-sensitive current. This indicates that a motif in the region 47–50 has a negative control on the channel activity and that residues in the region 68–79 are crucial for channel function. The deletion of residues 47–50 increases the channel current by increasing the number of channels at the cell surface (36).

Aldosterone is the main hormone controlling ENaC activity at the cell surface. The final step of regulation by aldosterone that leads to an increase in the number of active ENaCs at the cell surface remains unknown but might involve phosphorylation of the ENaC subunits. This question was addressed in Madin-Darby canine kidney cells transfected with $\alpha\beta\gamma$-ENaC subunits, and it was found that aldosterone, insulin, and protein kinases A and C increase the phosphorylation state of β- and γ- but not α-ENaC subunits (225). After aldosterone application, the increase in $\beta\gamma$-ENaC phosphorylation was already observed after 15 min and lasted over a 24-h period, indicating that this ENaC modification covers the early and late response of aldosterone. In this case, ENaC phosphorylation is associated with an increased ENaC activity at the cell surface. Recently phosphorylation of a conserved threonine residue in the close vicinity of the PY motif in β- (T613) and γ-ENaC (T623) subunits could be demonstrated in vivo in *Xenopus* oocytes (224). The functional relevance of these Thr residues is underlined by a three- to fourfold increase in channel activity after mutation of both residues to Ala or Glu. These results suggest that phosphorylation of the βT613 and γT623 likely by the extracellular regulated kinase (ERK kinase) downregulates ENaC at the cell surface by facilitating the interaction between the PY motif and Nedd4. Thus, depending on the target residue, phosphorylation of the COOH terminus of β- or γ-ENaC could either promote or decrease ENaC activity at the cell surface. The fact that phosphorylation inactivates Nedd4 as mentioned previously further adds to the complex role of the COOH terminus in the regulation of ENaC activity at the cell surface.

VIII. EPITHELIAL SODIUM CHANNEL MOLECULAR VARIANTS

PHA-I and Liddle's syndrome are inherited disorders of Na^+ balance due to ENaC mutations (described in sects. IIIA and VII). Homozygous mutations on the three $\alpha\beta\gamma$-ENaC subunits causing PHA-I have been identified that include premature stop codons [(numbering of human α ENaC) αR56stop, αR508stop], frameshift mutations (αI68fr, αT168fr, αF453fr, βT216fr, βD305fr), an abnormal γ-ENaC splice product at nucleotide 318 (238), and missense mutations (αC133Y and βG37S in human ENaC) (39, 95). Recently, the mutation of αS562, homologous to the selectivity filter residue (rat) αS589, to Leu has been found in a PHA-I patient (215). It is expected that truncation of α-ENaC at I68 which precedes M1 leads to a nonfunctional channel. In contrast, truncation of α-ENaC at αR508 leaves a protein with M1 and the major portion of the extracellular loop intact, that is able to assemble with β- and γ-subunits to be targeted to the cell membrane and to generate a small but detectable amiloride-sensitive current (27). This suggests that the αR508stop truncated protein retains sufficient information to promote subunit assembly and trafficking to the membrane. The residue βG37 is part of an intracellular domain that controls channel gating and has been discussed in section VIB of this review. Mutation of a conserved Cys in the post-M1 domain of αENaC to Tyr (human αENaC C133Y, corresponding to rat αENaC C158Y) also causes PHA-I. Functional analysis of this mutation introduced in rat αENaC (C158Y) coexpressed with $\beta\gamma$ wild-type ENaC in *Xenopus* oocytes showed that the mutant channel has very similar expression levels as wild-type when the oocytes are incubated at 19°C. If the oocytes are incubated at 30°C however, the Na^+ current of ENaC wild-type increases, whereas the current expression of the mutant decreases (95). The homologous C→S mutation in α-ENaC clearly decreases the current and cell surface expression in parallel even at 19°C, and this effect increases at higher temperature (77). Similarly, the analogous point mutation in β- and γ-ENaC decreases current expression. Because neither the assembly nor the degradation rate was affected by these mutants, it was suggested that the mutations may have introduced a Golgi retention signal as in the case for AQP-2 mutants causing nephrogenic diabetes insipidus (179).

The ENaC mutations causing Liddle's syndrome were very informative for the understanding of important structural and functional aspects of ENaC regulation (discussed in sect. VIIB). There was a remarkable correlation between the channel gain-of-function mutations identified by a systematic alanine scanning approach of the COOH terminus of β- and γ-ENaC (219) and the mutations found in Liddle's patients (105, 106, 114, 152, 218). Both the molecular screening and the genetic studies identified the

PPPxY motif (PY motif) in the β- and γ-ENaC as the target sequence for increased channel activity at the cell surface.

Because of the role of ENaC in Na^+ reabsorption and in the control of blood pressure, studies were undertaken to screen large numbers of hypertensive patients for mutations in the α-, β-, and γ-ENaC subunits. Particular attention was brought to exon 13 of ENaC genes where mutations in the PY motif causing Liddle's syndrome have been identified (see for review Ref. 48). In the COOH terminus, the polymorphisms αT663A, βG589S, βR597S, βR624C, βE623G, βT594M, γ594insP, γS613A, and γR631H (numbering of the human ENaC subunits) have been identified. ENaC variants in the extracellular loop include αA334, βA336P, βV434M, βG442V, γW177R, and γP501A. At present there is no evidence that any of these mutations affects ENaC function. Except for the αW493R variant, all these polymorphisms were found in regions of poorly conserved sequence. The αW493 residue is located ~50 residues NH_2-terminal of M2 in a highly conserved WPS motif found in all members of the ENaC/DEG family except for ASICs and FaNaC where W is replaced by I. The functional role of this WPS motif remains unknown. It remains possible that the *Xenopus* oocyte expression system is not consistent enough to detect small changes in channel activity for these variants, which may have smaller functional effects than the Liddle's variants which cause a greater than two- to threefold increase in channel activity. Other ENaC expression systems need to be developed to address the consequences of ENaC polymorphism on channel function to assess the role of ENaC in essential hypertension.

IX. PERSPECTIVES AND CONCLUSIONS

The molecular identification of ENaC, ASIC, and degenerin channels by functional cloning or genetic screening had a major impact on our understanding of transepithelial sodium transport, acid sensing in neurons, and mechanotransduction. Our knowledge regarding the structure and function of these channels is still emerging and needs to be improved. Important structural domains that form the channel core remain to be identified, in particular the structures participating in the inner channel pore. Solving the structure and determining the role of the large extracellular loop that constitutes more than one-half of the protein mass is of primary importance for our understanding of channel function. The functional heterogeneity among the ENaC/DEG family and the conservation of important functional domains provide at the same time a unique opportunity to address the molecular basis of channel functions such as activation by various stimuli or block by pharmacological ligands. We hope that in the near future the structure-function analysis as described in this review will be complemented by the determination of the three-dimensional structure of functional components of the channel protein.

There is increasing evidence that ENaC interacts with proteins that control its synthesis, membrane insertion, degradation, and function. It is possible that the functional ENaC complex found at the cell surface comprises in addition to the ENaC subunits other associated proteins similarly to the mechanotransduction complex in *C. elegans*. The analysis of regulatory pathways and of protein-protein interactions is in progress in the case of ENaC and will undoubtedly also help in understanding the function of other ENaC/DEG family members as, e.g., ASICs. In addition, strategies need to be developed to obtain a precise biochemical characterization of the functional channel complex at the cell surface and to identify possible associated proteins.

Inactivation of ASIC genes in animal models will hopefully clarify the physiological role of these acid-sensing channels in the central and peripheral nervous system. These models will certainly address the question whether a mechanotransducing system as found in *C. elegans* also exists in mammals or whether it remains confined to invertebrates. Inherited human diseases caused by the ENaC/DEG family members hINAC and ASICs have not been identified to date, but identification of such diseases would greatly help our understanding of the pathophysiological roles of these channels.

We thank J.-D. Horisberger for invaluable comments and discussions and B. C. Rossier, M. Driscoll, E. Lingueglia, L. Palmer, and P. Greasley for critical reading of the manuscript.

The work in the authors' laboratories was supported by Swiss National Science Foundation Grants 3100–059217.99 (to L. Schild) and 31–65233.01 (to S. Kellenberger) and Human Frontier Science Program Organization Grant RG0261 (to L. Schild). S. Kellenberger was supported by a National Institutes of Health Specialized Center of Research grant for hypertension.

Address for reprint requests and other correspondence: L. Schild, Institut de Pharmacologie et de Toxicologie, Bugnon 27, Université de Lausanne, CH-1005 Lausanne, Switzerland (E-mail: Laurent.Schild@ipharm.unil.ch).

REFERENCES

1. Abriel H and Horisberger JD. Feedback inhibition of rat amiloride-sensitive epithelial sodium channels expressed in *Xenopus laevis* oocytes. *J Physiol (Lond)* 516: 31–43, 1999.
2. Abriel H, Loffing J, Rebhun JF, Pratt JH, Schild L, Horisberger JD, Rotin D, and Staub O. Defective regulation of the epithelial Na^+ channel by Nedd4 in Liddle's syndrome. *J Clin Invest* 103: 667–673, 1999.
3. Adams CM, Anderson MG, Motto DG, Price MP, Johnson WA, and Welsh MJ. Ripped pocket and pickpocket, novel *Drosophila* Deg/ENaC subunits expressed in early development and in mechanosensory neurons. *J Cell Biol* 140: 143–152, 1998.
4. Adams CM, Snyder PM, Price MP, and Welsh MJ. Protons activate brain Na^+ channel 1 by inducing a conformational change that exposes a residue associated with neurodegeneration. *J Biol Chem* 273: 30204–30207, 1998.

5. Adams CM, Snyder PM, and Welsh MJ. Interactions between subunits of the human epithelial sodium channel. *J Biol Chem* 272: 27295–27300, 1997.
6. Adams CM, Snyder PM, and Welsh MJ. Paradoxical stimulation of a DEG/ENaC channel by amiloride. *J Biol Chem* 274: 15500–15504, 1999.
7. Akopian AN, Chen CC, Ding YN, Cesare P, and Wood JN. A new member of the acid-sensing ion channel family. *Neuroreport* 11: 2217–2222, 2000.
8. Askwith CC, Cheng C, Ikuma M, Benson C, Price MP, and Welsh MJ. Neuropeptide FF and FMRFamide potentiate acid-evoked currents from sensory neurons and proton-gated DEG/ENaC channels. *Neuron* 26: 133–141, 2000.
9. Avenet P and Lindemann B. Amiloride-blockable sodium currents in isolated taste receptor cells. *J Membr Biol* 105: 245–255, 1988.
10. Avenet P and Lindemann B. Fluctuation analysis of amiloride-blockable currents in membrane patches excised from salt-taste receptor cells. *J Basic Clin Physiol Pharmacol* 1: 383–391, 1990.
11. Awayda MS, Ismailov II, Berdiev BK, and Benos DJ. A cloned renal epithelial Na^+ channel protein displays stretch activation in planar lipid bilayers. *Am J Physiol Cell Physiol* 268: C1450–C1459, 1995.
12. Babinski K, Catarsi S, Biagini G, and Séguéla P. Mammalian ASIC2a and ASIC3 subunits co-assemble into heteromeric proton-gated channels sensitive to Gd^{3+}. *J Biol Chem* 275: 28519–28525, 2000.
13. Babinski K, Le KT, and Seguela P. Molecular cloning and regional distribution of a human proton receptor subunit with biphasic functional properties. *J Neurochem* 72: 51–57, 1999.
14. Barker PM, Gowen CW, Lawson EE, and Knowles MR. Decreased sodium ion absorption across nasal epithelium of very premature infants with respiratory distress syndrome. *J Pediatr* 130: 342–344, 1997.
15. Barker PM, Nguyen MS, Gatzy JT, Grubb B, Norman H, Hummler E, Rossier B, Boucher RC, and Koller B. Role of γ-ENaC subunit in lung liquid clearance and electrolyte balance in newborn mice. *J Clin Invest* 102: 1634–1640, 1998.
16. Baron A, Schaefer L, Lingueglia E, Champigny G, and Lazdunski M. Zn^{2+} and H^+ are coactivators of acid-sensing ion channels. *J Biol Chem* 276: 35361–35367, 2001.
17. Bassilana F, Champigny G, Waldmann R, Deweille JR, Heurteaux C, and Lazdunski M. The acid-sensitive ionic channel subunit ASIC and the mammalian degenerin MDEG form a heteromultimeric H^+-gated Na^+ channel with novel properties. *J Biol Chem* 272: 28819–28822, 1997.
18. Bassler EL, Ngo-Anh TJ, Geisler HS, Ruppersberg JP, and Grunder S. Molecular and functional characterization of acid-sensing ion channel (ASIC) 1b. *J Biol Chem* 276: 33782–33787, 2001.
19. Belkin KJ and Abrams TW. FMRFamide produces biphasic modulation of the LFS motor neurons in the neural circuit of the siphon withdrawal reflex of *Aplysia* by activating Na^+ and K^+ currents. *J Neurosci* 13: 5139–5152, 1993.
20. Benos DJ. Amiloride: a molecular probe of sodium transport in tissues and cells. *Am J Physiol Cell Physiol* 242: C131–C145, 1982.
21. Benos DJ, Awayda MS, Berdiev BK, Bradford AL, Fuller CM, Senyk O, and Ismailov II. Diversity and regulation of amiloride-sensitive Na^+ channels. *Kidney Int* 49: 1632–1637, 1996.
22. Benos DJ, Fuller CM, Shlyonsky VG, Berdiev BK, and Ismailov II. Amiloride-sensitive Na^+ channels: insights and outlooks. *News Physiol Sci* 12: 55–61, 1997.
23. Benson CJ, Eckert SP, and McCleskey EW. Acid-evoked currents in cardiac sensory neurons: a possible mediator of myocardial ischemic sensation. *Circ Res* 84: 921–928, 1999.
24. Berdiev BK, Prat AG, Cantiello HF, Ausiello DA, Fuller CM, Jovov B, Benos DJ, and Ismailov II. Regulation of epithelial sodium channels by short actin filaments. *J Biol Chem* 271: 17704–17710, 1996.
25. Bevan S and Yeats J. Protons activate a cation conductance in a subpopulation of rat dorsal root ganglion neurones. *J Physiol* 433: 145–161, 1991.
26. Biagini G, Babinski K, Avoli M, Marcinkiewicz M, and Seguela P. Regional and subunit-specific downregulation of acid-sensing ion channels in the pilocarpine model of epilepsy. *Neurobiol Dis* 8: 45–58, 2001.
27. Bonny O, Chraibi A, Loffing J, Jaeger NF, Grunder S, Horisberger JD, and Rossier BC. Functional expression of a pseudohypoaldosteronism type I mutated epithelial Na^+ channel lacking the pore-forming region of its alpha subunit. *J Clin Invest* 104: 967–974, 1999.
28. Bradford AL, Ismailov II, Achard JM, Warnock DG, Bubien JK, and Benos DJ. Immunopurification and functional reconstitution of a Na^+ channel complex from rat lymphocytes. *Am J Physiol Cell Physiol* 269: C601–C611, 1995.
29. Brouard M, Casado M, Djelidi S, Barrandon Y, and Farman N. Epithelial sodium channel in human epidermal keratinocytes: expression of its subunits and relation to sodium transport and differentiation. *J Cell Sci* 112: 3343–3352, 1999.
30. Burch LH, Talbot CR, Knowles MR, Canessa CM, Rossier BC, and Boucher RC. Relative expression of the human epithelial Na^+ channel subunits in normal and cystic fibrosis airways. *Am J Physiol Cell Physiol* 269: C511–C518, 1995.
31. Canessa CM, Horisberger JD, and Rossier BC. Epithelial sodium channel related to proteins involved in neurodegeneration. *Nature* 361: 467–470, 1993.
32. Canessa CM, Merillat AM, and Rossier BC. Membrane topology of the epithelial sodium channel in intact cells. *Am J Physiol Cell Physiol* 267: C1682–C1690, 1994.
33. Canessa CM, Schild L, Buell G, Thorens B, Gautschi I, Horisberger JD, and Rossier BC. Amiloride-sensitive epithelial Na^+ channel is made of three homologous subunits. *Nature* 367: 463–467, 1994.
34. Catarsi S, Babinski K, and Seguela P. Selective modulation of heteromeric ASIC proton-gated channels by neuropeptide FF. *Neuropharmacology* 41: 592–600, 2001.
35. Chalfant ML, Denton JS, Berdiev BK, Ismailov II, Benos DJ, and Stanton BA. Intracellular H^+ regulates the alpha-subunit of ENaC, the epithelial Na^+ channel. *Am J Physiol Cell Physiol* 276: C477–C486, 1999.
36. Chalfant ML, Denton JS, Langloh AL, Karlson KH, Loffing J, Benos DJ, and Stanton BA. The NH_2 terminus of the epithelial sodium channel contains an endocytic motif. *J Biol Chem* 274: 32889–32896, 1999.
37. Chalfie M and Au M. Genetic control of differentiation of the *Caenorhabditis elegans* touch receptor neurons. *Science* 243: 1027–1033, 1989.
38. Champigny G, Voilley N, Waldmann R, and Lazdunski M. Mutations causing neurodegeneration in *Caenorhabditis elegans* drastically alter the pH sensitivity and inactivation of the mammalian H^+-gated Na^+ channel MDEG1. *J Biol Chem* 273: 15418–15422, 1998.
39. Chang S, Grunder S, Hanukoglu A, Rosler A, Mathew P, Hanukoglu I, Schild L, Lu Y, Shimkets R, Nelson-Williams C, Rossier BC, and Lifton RP. Mutations in subunits of the epithelial sodium channel cause salt wasting with hyperkalaemic acidosis, pseudohypoaldosteronism type 1. *Nature Genet* 12: 248–53, 1996.
40. Chen CC, England S, Akopian AN, and Wood JN. A sensory neuron-specific, proton-gated ion channel. *Proc Natl Acad Sci USA* 95: 10240–10245, 1998.
41. Chen L, Reif MC, and Schafer JA. Clonidine and PGE_2 have different effects on Na^+ and water transport in rat and rabbit CCD. *Am J Physiol Renal Fluid Electrolyte Physiol* 261: F126–F136, 1991.
42. Chen SY, Bhargava A, Mastroberardino L, Meijer OC, Wang J, Buse P, Firestone GL, Verrey F, and Pearce D. Epithelial sodium channel regulated by aldosterone-induced protein sgk. *Proc Natl Acad Sci USA* 96: 2514–2519, 1999.
43. Chesler M. The regulation and modulation of pH in the nervous system. *Prog Neurobiol* 34: 401–427, 1990.
44. Chesler M and Kaila K. Modulation of pH by neuronal activity. *Trends Neurosci* 15: 396–402, 1992.
45. Chow YH, Wang Y, Plumb J, O'Brodovich H, and Hu J. Hormonal regulation and genomic organization of the human amiloride-sensitive epithelial sodium channel alpha subunit gene. *Pediatr Res* 46: 208–214, 1999.
46. Chraibi A, Vallet V, Firsov D, Hess SK, and Horisberger JD. Protease modulation of the activity of the epithelial sodium channel expressed in *Xenopus* oocytes. *J Gen Physiol* 111: 127–138, 1998.
47. Chraibi A, Verdumo C, Merillat AM, Rossier BC, Horisberger JD, and Hummler E. Functional analyses of a N-terminal splice variant

of the α subunit of the epithelial sodium channel. *Cell Physiol Biochem* 11: 115–122, 2001.
48. Corvol P, Persu A, Gimenez-Roqueplo AP, and Jeunemaitre X. Seven lessons from two candidate genes in human essential hypertension: angiotensinogen and epithelial sodium channel. *Hypertension* 33: 1324–1331, 1999.
49. Coscoy S, deWeille JR, Lingueglia E, and Lazdunski M. The pretransmembrane 1 domain of acid-sensing ion channels participates in the ion pore. *J Biol Chem* 274: 10129–10132, 1999.
50. Coscoy S, Lingueglia E, Lazdunski M, and Barbry P. The phe-met-arg-phe-amide-activated sodium channel is a tetramer. *J Biol Chem* 273: 8317–8322, 1998.
51. Cottrell GA. The first peptide-gated ion channel. *J Exp Biol* 200: 2377–2386, 1997.
52. Cottrell GA, Jeziorski MC, and Green KA. Location of a ligand recognition site of FMRFamide-gated Na^+ channels. *FEBS Lett* 489: 71–74, 2001.
53. Couloigner V, Fay M, Djelidi S, Farman N, Escoubet B, Runembert I, Sterkers O, Friedlander G, and Ferrary E. Location and function of the epithelial Na channel in the cochlea. *Am J Physiol Renal Physiol* 280: F214–F222, 2001.
54. Dagenais A, Kothary R, and Berthiaume Y. The α subunit of the epithelial sodium channel in the mouse: developmental regulation of its expression. *Pediatr Res* 42: 327–334, 1997.
55. Darboux I, Lingueglia E, Champigny G, Coscoy S, Barbry P, and Lazdunski M. Dgnac1, a gonad-specific amiloride-sensitive Na^+ channel. *J Biol Chem* 273: 9424–9429, 1998.
56. Darboux I, Lingueglia E, Pauron D, Barbry P, and Lazdunski M. A new member of the amiloride-sensitive sodium channel family in *Drosophila melanogaster* peripheral nervous system. *Biochem Biophys Res Commun* 246: 210–216, 1998.
57. Davis RE and Stretton AO. The motornervous system of *Ascaris*: electrophysiology and anatomy of the neurons and their control by neuromodulators. *Parasitology* 113: 97–117, 1996.
58. Debonneville C, Flores SY, Kamynina E, Plant PJ, Tauxe C, Thomas MA, Munster C, Chraibi A, Pratt JH, Horisberger, JD, Pearce D, Loffing J, and Staub C. Phosphorylation of Nedd4–2 by Sgk1 regulates epithelial Na^+ channel cell surface expression. *EMBO J* 20: 7052–7059, 2001.
59. De la Rosa DA, Zhang P, Naray-Fejes-Toth A, Fejes-Toth G, and Canessa CM. The serum and glucocorticoid kinase sgk increases the abundance of epithelial sodium channels in the plasma membrane of *Xenopus* oocytes. *J Biol Chem* 274: 37834–37839, 1999.
60. DeWeille J and Bassilana F. Dependence of the acid-sensitive ion channel, ASIC1a, on extracellular Ca^{2+} ions. *Brain Res* 900: 277–281, 2001.
61. DeWeille JR, Bassilana FR, Lazdunski M, and Waldmann R. Identification, functional expression and chromosomal localisation of a sustained human proton-gated cation channel. *FEBS Lett* 433: 257–260, 1998.
62. Dijkink L, Hartog A, Van Os CH, and Bindels RJM. Modulation of aldosterone-induced stimulation of ENaC synthesis by changing the rate of apical Na^+ entry. *Am J Physiol Renal Physiol* 281: F687–F692, 2001.
63. Dinudom A, Young JA, and Cook DI. Amiloride-sensitive Na^+ current in the granular duct cells of mouse mandibular glands. *Pflügers Arch* 423: 164–166, 1993.
64. Doyle DA, Cabral JM, Pfuetzner RA, Kuo AL, Gulbis JM, Cohen SL, Chait BT, and MacKinnon R. The structure of the potassium channel: molecular basis of K^+ conduction and selectivity. *Science* 280: 69–77, 1998.
65. Driscoll M and Chalfie M. The *mec-4* gene is a member of a family of *Caenorhabditis elegans* genes that can mutate to induce neuronal degeneration. *Nature* 349: 588–593, 1991.
66. Drummond HA, Abboud FM, and Welsh MJ. Localization of beta and gamma subunits of ENaC in sensory nerve endings in the rat foot pad. *Brain Res* 884: 1–12, 2000.
67. Drummond HA, Price MP, Welsh MJ, and Abboud FM. A molecular component of the arterial baroreceptor mechanotransducer. *Neuron* 21: 1435–1441, 1998.
68. Du HP, Gu GQ, William CM, and Chalfie M. Extracellular proteins needed for *C. elegans* mechanosensation. *Neuron* 16: 183–194, 1996.
69. Duc C, Farman N, Canessa CM, Bonvalet JP, and Rossier BC. Cell-specific expression of epithelial sodium channel α, β, and γ subunits in aldosterone-responsive epithelia from the rat: localization by in situ hybridization and immunocytochemistry. *J Cell Biol* 127: 1907–1921, 1994.
70. Duggan A, Garcia-Anoveros J, and Corey DP. Insect mechanoreception: what a long, strange TRP it's been. *Curr Biol* 10: R384–R387, 2000.
71. Epple HJ, Amasheh S, Mankertz J, Goltz M, Schulzke JD, and Fromm M. Early aldosterone effect in distal colon by transcriptional regulation of ENaC subunits. *Am J Physiol Gastrointest Liver Physiol* 278: G718–G724, 2000.
72. Escoubas P, DeWeille JR, Lecoq A, Diochot S, Waldmann R, Champigny G, Moinier D, Ménez A, and Lazdunski M. Isolation of a tarantula toxin specific for a class of proton-gated Na^+ channels. *J Biol Chem* 275: 25116–25121, 2000.
73. Eskandari S, Snyder PM, Kreman M, Zampighi GA, Welsh MJ, and Wright EM. Number of subunits comprising the epithelial sodium channel. *J Biol Chem* 274: 27281–27286, 1999.
74. Farman N, Talbot CR, Boucher R, Fay M, Canessa C, Rossier B, and Bonvalet JP. Noncoordinated expression of α, β, and γ subunit mRNAs of epithelial Na^+ channel along rat respiratory tract. *Am J Physiol Cell Physiol* 272: C131–C141, 1997.
75. Ferreira J, Santos AR, and Calixto JB. Antinociception produced by systemic, spinal and supraspinal administration of amiloride in mice. *Life Sci* 65: 1059–1066, 1999.
76. Firsov D, Gautschi I, Merillat AM, Rossier BC, and Schild L. The heterotetrameric architecture of the epithelial sodium channel (ENaC). *EMBO J* 17: 344–352, 1998.
77. Firsov D, Robert-Nicoud M, Gruender S, Schild L, and Rossier BC. Mutational analysis of cysteine-rich domains of the epithelium sodium channel (ENaC): identification of cysteines essential for channel expression at the cell surface. *J Biol Chem* 274: 2743–2749, 1999.
78. Firsov D, Schild L, Gautschi I, Merillat AM, Schneeberger E, and Rossier BC. Cell surface expression of the epithelial Na channel and a mutant causing Liddle syndrome: a quantitative approach. *Proc Natl Acad Sci USA* 93: 15370–15375, 1996.
79. Frindt G and Palmer LG. Regulation of Na channels in the rat cortical collecting tubule: effects of cAMP and methyl donors. *Am J Physiol Renal Fluid Electrolyte Physiol* 271: F1086–F1092, 1996.
80. Frindt G, Silver RB, Windhager EE, and Palmer LG. Feedback regulation of Na channels in rat CCT. II. Effects of inhibition of Na entry. 264: F565–F574, 1993.
81. Fuller CM, Berdiev BK, Shlyonsky VG, Ismailov II, and Benos DJ. Point mutations in alpha benac regulate channel gating, ion selectivity, and sensitivity to amiloride. *Biophys J* 72: 1622–1632, 1997.
82. Garcia-Anoveros J and Corey DP. The molecules of mechanosensation. *Annu Rev Neurosci* 20: 567–594, 1997.
83. Garcia-Anoveros J, Derfler B, Nevillegolden J, Hyman BT, and Corey DP. BNaC1 and BNaC2 constitute at new family of human neuronal sodium channels related to degenerins and epithelial sodium channels. *Proc Natl Acad Sci USA* 94: 1459–1464, 1997.
84. Garcia-Anoveros J, Garcia JA, Liu JD, and Corey DP. The nematode degenerin UNC-105 forms ion channels that are activated by degeneration- or hypercontraction-causing mutations. *Neuron* 20: 1231–1241, 1998.
85. Garcia-Anoveros J, Ma C, and Chalfie M. Regulation of *Caenorhabditis elegans* degenerin proteins by a putative extracellular domain. *Curr Biol* 5: 441–448, 1995.
86. Garcia-Anoveros J, Samad TA, Zuvela-Jelaska L, Woolf CJ, and Corey DR. Transport and localization of the DEG/ENaC ion channel BNaC1 alpha to peripheral mechanosensory terminals of dorsal root ganglia neurons. *J Neurosci* 21: 2678–2686, 2001.
87. Garty H and Palmer LG. Epithelial sodium channels: function, structure, and regulation. *Physiol Rev* 77: 359–396, 1997.
88. Gillespie PG and Walker RG. Molecular basis of mechanosensory transduction. *Nature* 413: 194–202, 2001.
89. Golestaneh N, Nicolas C, Picaud S, Ferrari P, and Mirshahi M. The epithelial sodium channel (ENaC) in rodent retina, ontogeny and molecular identity. *Curr Eye Res* 21: 703–709, 2000.
90. Goodman MB, Ernstrom GG, Chelur DS, O'Hagan R, Yao CA, and

CHALFIE M. MEC2 regulates *C. elegans* DEG/ENaC channels needed for mechanosensation. *Nature* 415: 1039–1042, 2002.
91. GOODMAN MB, HALL DH, AVERY L, AND LOCKERY SR. Active currents regulate sensitivity and dynamic range in C. *elegans* neurons. *Neuron* 20: 763–772, 1998.
92. GRANTYN R AND LUX HD. Similarity and mutual exclusion of NMDA- and proton-activated transient Na^+ currents in rat tectal neurons. *Neurosci Lett* 98: 198–203, 1988.
93. GREEN KA AND COTTRELL GA. Block of the helix FMRFamide-gated Na^+ channel by FMRFamide and its analogues. *J Physiol* 519: 47–56, 1999.
94. GREEN KA, FALCONER SW, AND COTTRELL GA. The neuropeptide Phe-Met-Arg-Phe-NH_2 (FMRFamide) directly gates two ion channels in an identified *Helix* neurone. *Pflügers Arch* 428: 232–240, 1994.
95. GRUNDER S, CHANG SS, LIFTON R, AND ROSSIER BC. PHA-1: a novel thermosensitive mutation in the ectodomain of αENaC (Abstract). *J Am Soc Nephrol* 9: A0178, 1998.
96. GRUNDER S, FIRSOV D, CHANG SS, JAEGER NF, GAUTSCHI I, SCHILD L, LIFTON RP, AND ROSSIER BC. A mutation causing pseudohypoaldosteronism type 1 identifies a conserved glycine that is involved in the gating of the epithelial sodium channel. *EMBO J* 16: 899–907, 1997.
97. GRÜNDER S, GEISSLER HS, BÄSSLER EL, AND RUPPERSBERG JP. A new member of acid-sensing ion channels from pituitary gland. *Neuroreport* 11: 1607–1611, 2000.
98. GRUNDER S, JAEGER NF, GAUTSCHI I, SCHILD L, AND ROSSIER BC. Identification of a highly conserved sequence at the N-terminus of the epithelial Na^+ channel alpha subunit involved in gating. *Pflügers Arch* 438: 709–715, 1999.
99. GRÜNDER S, MÜLLER A, AND RUPPERSBERG JP. Developmental and cellular expression pattern of epithelial sodium channel α, β and γ subunits in the inner ear of the rat. *Eur J Neurosci* 13: 641–648, 2001.
100. GU G, CALDWELL GA, AND CHALFIE M. Genetic interactions affecting touch sensitivity in *Caenorhabditis elegans*. *Proc Natl Acad Sci USA* 93: 6577–6582, 1996.
101. HALL DH, GU GQ, GARCIA-ANOVEROS J, GONG L, CHALFIE M, AND DRISCOLL M. Neuropathology of degenerative cell death in *Caenorhabditis elegans*. *J Neurosci* 17: 1033–1045, 1997.
102. HAMILL OP AND MARTINAC B. Molecular basis of mechanotransduction in living cells. *Physiol Rev* 81: 685–740, 2001.
103. HAMILL OP AND MCBRIDE DW JR. The pharmacology of mechanogated membrane ion channels. *Pharmacol Rev* 48: 231–252, 1996.
104. HAMILTON KL AND EATON DC. Single-channel recordings from amiloride-sensitive epithelial sodium channel. *Am J Physiol Cell Physiol* 249: C200–C207, 1985.
105. HANSSON JH, NELSON-WILLIAMS C, SUZUKI H, SCHILD L, SHIMKETS R, LU Y, CANESSA C, IWASAKI T, ROSSIER B, AND LIFTON RP. Hypertension caused by a truncated epithelial sodium channel gamma subunit: genetic heterogeneity of Liddle syndrome. *Nature Genet* 11: 76–82, 1995.
106. HANSSON JH, SCHILD L, LU Y, WILSON TA, GAUTSCHI I, SHIMKETS R, NELSON-WILLIAMS C, ROSSIER BC, AND LIFTON RP. A de novo missense mutation of the β subunit of the epithelial sodium channel causes hypertension and Liddle syndrome, identifying a proline-rich segment critical for regulation of channel activity. *Proc Natl Acad Sci USA* 92: 11495–11499, 1995.
107. HILLE B. *Ionic Channels of Excitable Membranes*. Sunderland, MA: Sinauer, 1992.
108. HONG K AND DRISCOLL M. A transmembrane domain of the putative channel subunit MEC-4 influences mechanotransduction and neurodegeneration in *C. elegans*. *Nature* 367: 470–473, 1994.
109. HONG K, MANO I, AND DRISCOLL M. In vivo structure-function analyses of *Caenorhabditis elegans* MEC-4, a candidate mechanosensory ion channel subunit. *J Neurosci* 20: 2575–2588, 2000.
110. HUANG M AND CHALFIE M. Gene interactions affecting mechanosensory transduction in *Caenorrhabditis elegans*. *Nature* 367: 467–470, 1994.
111. HUMMLER E, BARKER P, GATZY J, BEERMANN F, VERDUMO C, SCHMIDT A, BOUCHER RC, AND ROSSIER BC. Early death due to defective neonatal lung liquid clearance in αENaC-deficient mice. *Nature Genet* 12: 325–328, 1996.
112. HUMMLER E, BARKER P, TALBOT C, WANG Q, VERDUMO C, GRUBB B, GATZY J, BURNIER M, HORISBERGER JD, BEERMANN F, BOUCHER R, AND ROSSIER BC. A mouse model for the renal salt-wasting syndrome pseudohypoaldosteronism. *Proc Natl Acad Sci USA* 94: 11710–11715, 1997.
113. IMMKE DC AND MCCLESKEY EW. Lactate enhances the acid-sensing Na^+ channel on ischemia-sensing neurons. *Nat Neurosci* 4: 869–870, 2001.
114. INOUE J, IWAOKA T, TOKUNAGA H, TAKAMUNE K, NAOMI S, ARAKI M, TAKAHAMA K, YAMAGUCHI K, AND TOMITA K. A family with Liddles-syndrome caused by a new missense mutation in the β subunit of the epithelial sodium channel. *J Clin Endocrinol Metab* 83: 2210–2213, 1998.
115. INOUE T, NONOGUCHI H, AND TOMITA K. Physiological effects of vasopressin and atrial natriuretic peptide in the collecting duct. *Cardiovasc Res* 51: 470–80, 2001.
116. ISHIBASHI K AND MARUMO F. Molecular cloning of a Deg/Enac sodium channel cDNA from human testis. *Biochem Biophys Res Commun* 245: 589–593, 1998.
117. ISHIKAWA T, MARUNAKA Y, AND ROTIN D. Electrophysiological characterization of the rat epithelial Na^+ channel (rENaC) expressed in MDCK cells: effects of Na^+ and Ca^{2+}. *J Gen Physiol* 111: 825–846, 1998.
118. ISMAILOV II, AWAYDA MS, BERDIEV BK, BUBIEN JK, LUCAS JE, FULLER CM, AND BENOS DJ. Triple-barrel organization of ENaC, a cloned epithelial Na^+ channel. *J Biol Chem* 271: 807–816, 1996.
119. ISMAILOV II, AWAYDA MS, JOVOV B, BERDIEV BK, FULLER CM, DEDMAN JR, KAETZEL MA, AND BENOS DJ. Regulation of epithelial sodium channels by the cystic fibrosis transmembrane conductance regulator. *J Biol Chem* 271: 4725–4732, 1996.
120. ISMAILOV II AND BENOS DJ. Effects of phosphorylation on ion channel function. *Kidney Int* 48: 1167–1179, 1995.
121. ISMAILOV II, BERDIEV BK, AND BENOS DJ. Biochemical status of renal epithelial Na^+ channels determines apparent channel conductance, ion selectivity, and amiloride sensitivity. *Biophys J* 69: 1789–1800, 1995.
122. ISMAILOV II, BERDIEV BK, AND BENOS DJ. Regulation by Na^+ and Ca^{2+} of renal epithelial Na^+ channels reconstituted into planar lipid bilayers. *J Gen Physiol* 106: 445–466, 1995.
123. ISMAILOV II, BERDIEV BK, SHLYONSKY VG, AND BENOS DJ. Mechanosensitivity of an epithelial Na^+ channel in planar lipid bilayers: release from Ca^{2+} block. *Biophys J* 72: 1182–1192, 1997.
124. ISMAILOV II, BERDIEV BK, SHLYONSKY VG, FULLER CM, PRAT AG, JOVOV B, CANTIELLO HF, AUSIELLO DA, AND BENOS DJ. Role of actin in regulation of epithelial sodium channels by CFTR. *Am J Physiol Cell Physiol* 272: C1077–C1086, 1997.
125. ISMAILOV II, KIEBER-EMMONS T, LIN CM, BERDIEV BK, SHLYONSKY VG, PATTON HK, FULLER CM, WORRELL R, ZUCKERMAN JB, SUN W, EATON DC, BENOS DJ, AND KLEYMAN TR. Identification of an amiloride binding domain within the alpha-subunit of the epithelial Na^+ channel. *J Biol Chem* 272: 21075–21083, 1997.
126. IWASAKI K, LIU DW, AND THOMAS JH. Genes that control a temperature-compensated ultradian clock in *Caenorhabditis elegans*. *Proc Natl Acad Sci USA* 92: 10317–10321, 1995.
127. JEZIORSKI MC, GREEN KA, SOMMERVILLE J, AND COTTRELL GA. Cloning and expression of a FMRFamide-gated Na^+ channel from *Helisoma trivolvis* and comparison with the native neuronal channel. *J Physiol* 526: 13–25, 2000.
128. JI HL, PARKER S, LANGLOH ALB, FULLER CM, AND BENOS DJ. Point mutations in the post-M2 region of human alpha-ENaC regulate cation selectivity. *Am J Physiol Cell Physiol* 281: C64–C74, 2001.
129. JOHNSON MB, JIN K, MINAMI M, CHEN D, AND SIMON RP. Global ischemia induces expression of acid-sensing ion channel 2a in rat brain. *J Cereb Blood Flow Metab* 21: 734–740, 2001.
130. JOVOV B, TOUSSON A, JI HL, KEETON D, SHLYONSKY V, RIPOLL PJ, FULLER CM, AND BENOS DJ. Regulation of epithelial Na^+ channels by actin in planar lipid bilayers and in the *Xenopus* oocyte expression system. *J Biol Chem* 274: 37845–37854, 1999.
131. JULIUS D AND BASBAUM AI. Molecular mechanisms of nociception. *Nature* 413: 203–210, 2001.
132. KAMYNINA E, DEBONNEVILLE C, BENS M, VANDEWALLE A, AND STAUB O. A novel mouse Nedd4 protein suppresses the activity of the epithelial Na^+ channel. *FASEB J* 15: 204–214, 2001.

133. KANELIS V, ROTIN D, AND FORMAN-KAY JD. Solution structure of a Nedd4 WW domain-ENaC peptide complex. *Nature Struct Biol* 8: 407–412, 2001.
134. KATSURA I, KONDO K, AMANO T, ISHIHARA T, AND KAWAKAMI M. Isolation, characterization and epistasis of fluoride-resistant mutants of *Caenorhabditis elegans*. *Genetics* 136: 145–154, 1994.
135. KELLENBERGER S, AUBERSON M, GAUTSCHI I, SCHNEEBERGER E, AND SCHILD L. Permeability properties of ENaC selectivity filter mutants. *J Gen Physiol* 118: 679–692, 2001.
136. KELLENBERGER S, GAUTSCHI I, ROSSIER BC, AND SCHILD L. Mutations causing Liddle syndrome reduce sodium-dependent downregulation of the epithelial sodium channel in the *Xenopus* oocyte expression system. *J Clin Invest* 101: 2741–2750, 1998.
137. KELLENBERGER S, GAUTSCHI I, AND SCHILD L. A single point mutation in the pore region of the epithelial Na^+ channel changes ion selectivity by modifying molecular sieving. *Proc Natl Acad Sci USA* 96: 4170–4175, 1999.
138. KELLENBERGER S, HOFFMANN-POCHON N, GAUTSCHI I, SCHNEEBERGER E, AND SCHILD L. On the molecular basis of ion permeation in the epithelial Na^+ channel. *J Gen Physiol* 114: 13–30, 1999.
139. KEREM E, BISTRITZER T, HANUKOGLU A, HOFMANN T, ZHOU Z, BENNETT W, MACLAUGHLIN E, BARKER P, NASH M, QUITTELL L, BOUCHER R, AND KNOWLES MR. Pulmonary epithelial sodium-channel dysfunction and excess airway liquid in pseudohypoaldosteronism. *N Engl J Med* 341: 156–162, 1999.
140. KHAKH BS, BAO XR, LABARCA C, AND LESTER HA. Neuronal P2X transmitter-gated cation channels change their ion selectivity in seconds. *Nature Neurosci* 2: 322–330, 1999.
141. KIEBER-EMMONS T, LIN C, FOSTER MH, AND KLEYMAN TR. Antiidiotypic antibody recognizes an amiloride binding domain within the alpha subunit of the epithelial Na^+ channel. *J Biol Chem* 274: 9648–9655, 1999.
142. KILLICK R AND RICHARDSON G. Isolation of chicken alpha ENaC splice variants from a cochlear cDNA library. *Biochim Biophys Acta* 1350: 33–37, 1997.
143. KLEYMAN TR AND CRAGOE EJ JR. Amiloride and its analogs as tools in the study of ion transport. *J Membr Biol* 105: 1–21, 1988.
144. KOEFOED-JOHNSON V AND USSING HH. On the nature of the frog skin potential. *Acta Physiol Scand* 42: 298–308, 1958.
145. KOREN G, LIMAN ER, LOGOTHETIS DE, NADAL-GINARD B, AND HESS P. Gating mechanism of a cloned potassium channel expressed in frog oocytes and mammalian cells. *Neuron* 4: 39–51, 1990.
146. KOSARI F, SHENG SH, LI JQ, MAK DD, FOSKETT JK, AND KLEYMAN TR. Subunit stoichiometry of the epithelial sodium channel. *J Biol Chem* 273: 13469–13474, 1998.
147. KRETZ O, BARBRY P, BOCK R, AND LINDEMANN B. Differential expression of mRNA and protein of the three pore-forming subunits of the amiloride-sensitive epithelial sodium channel in taste buds of the rat. *J Histochem Cytochem* 47: 51–64, 1999.
148. KRISHTAL OA AND PIDOPLICHKO VI. A receptor for protons in the membrane of sensory neurons may participate in nociception. *Neuroscience* 6: 2599–2601, 1981.
149. KROVETZ HS, VANDONGEN HMA, AND VANDONGEN AMJ. Atomic distance estimates from disulfides and high-affinity metal-binding sites in a K^+ channel pore. *Biophys J* 72: 117–126, 1997.
150. LEWIS SA, EATON DC, AND DIAMOND JM. The mechanism of Na^+ transport by rabbit urinary bladder. *J Membr Biol* 28: 41–70, 1976.
151. LI XJ, XU RH, GUGGINO WB, AND SNYDER SH. Alternatively spliced forms of the α subunit of the epithelial sodium channel: distinct sites for amiloride binding and channel pore. *Mol Pharmacol* 47: 1133–1140, 1995.
152. LIFTON RP. Genetic determinants of human hypertension. *Proc Natl Acad Sci USA* 92: 8545–8551, 1995.
153. LIFTON RP, GHARAVI AG, AND GELLER DS. Molecular mechanisms of human hypertension. *Cell* 104: 545–556, 2001.
154. LIN W, FINGER TE, ROSSIER BC, AND KINNAMON SC. Epithelial Na^+ channel subunits in rat taste cells: localization and regulation by aldosterone. *J Comp Neurol* 405: 406–420, 1999.
155. LINDEMANN B. Taste reception. *Physiol Rev* 76: 718–766, 1996.
156. LINDEMANN B. Receptors and transduction in taste. *Nature* 413: 219–225, 2001.
157. LINGUEGLIA E, CHAMPIGNY G, LAZDUNSKI M, AND BARBRY P. Cloning of the amiloride-sensitive FMRFamide peptide-gated sodium channel. *Nature* 378: 730–733, 1995.
158. LINGUEGLIA E, DEWEILLE JR, BASSILANA F, HEURTEAUX C, SAKAI H, WALDMANN R, AND LAZDUNSKI M. A modulatory subunit of acid sensing ion channels in brain and dorsal root ganglion cells. *J Biol Chem* 272: 29778–29783, 1997.
159. LINGUEGLIA E, VOILLEY N, WALDMANN R, LAZDUNSKI M, AND BARBRY P. Expression cloning of an epithelial amiloride-sensitive Na^+ channel. *FEBS Lett* 318: 95–99, 1993.
160. LIPKIND GM AND FOZZARD HA. KcsA crystal structure as framework for a molecular model of the Na^+ channel pore. *Biochemistry* 39: 8161–8170, 2000.
161. LIPTON P. Ischemic cell death in brain neurons. *Physiol Rev* 79: 1431–1568, 1999.
162. LITTLETON JT AND GANETZKY B. Ion channels and synaptic organization: analysis of the *Drosophila* genome. *Neuron* 26: 35–43, 2000.
163. LIU JD, SCHRANK B, AND WATERSTON RH. Interaction between a putative mechanosensory membrane channel and a collagen. *Science* 273: 361–364, 1996.
164. LIU L AND SIMON SA. Capsaicin, acid and heat-evoked currents in rat trigeminal ganglion neurons. Relationship to functional VR1 receptors. *Physiol Behav* 69: 363–378, 2000.
165. LOCKERY SR AND GOODMAN MB. Tight-seal whole-cell patch clamping of *Caenorhabditis elegans* neurons. *Methods Enzymol* 293: 201–217, 1998.
166. LOFFING J, LOFFING-CUENI D, MACHER A, HEBERT SC, OLSON B, KNEPPER MA, ROSSIER BC, AND KAISSLING B. Localization of epithelial sodium channel and aquaporin-2 in rabbit kidney cortex. *Am J Physiol Renal Physiol* 278: F530–F539, 2000.
167. LOFFING J, PIETRI L, AREGGER F, BLOCH-FAURE M, ZIEGLER U, MENETON P, ROSSIER BC, AND KAISSLING B. Differential subcellular localization of ENaC subunits in mouse kidney in response to high- and low-Na diets. *Am J Physiol Renal Physiol* 279: F252–F258, 2000.
168. LOFFING J, ZECEVIC M, FERAILLE E, KAISSLING B, ASHER C, ROSSIER BC, FIRESTONE GL, PEARCE D, AND VERREY F. Aldosterone induces rapid apical translocation of ENaC in early portion of renal collecting system: possible role of SGK. *Am J Physiol Renal Physiol* 280: F675–F682, 2001.
169. LUDWIG M, BOLKENIUS U, WICKERT L, MARYNEN P, AND BIDLINGMAIER F. Structural organisation of the gene encoding the alpha-subunit of the human amiloride-sensitive epithelial sodium channel. *Hum Genet* 102: 576–581, 1998.
170. MACKINNON R. Determination of the subunit stoichiometry of a voltage-activated potassium channel. *Nature* 350: 232–235, 1991.
171. MANO I AND DRISCOLL M. DEG/ENaC channels: a touchy superfamily that watches its salt. *Bioessays* 21: 568–578, 1999.
172. MASILAMANI S, KIM GH, MITCHELL C, WADE JB, AND KNEPPER MA. Aldosterone-mediated regulation of ENaC alpha, beta, and gamma subunit proteins in rat kidney. *J Clin Invest* 104: R19–R23, 1999.
173. MATSUSHITA K, MCCRAY PB JR, SIGMUND RD, WELSH MJ, AND STOKES JB. Localization of epithelial sodium channel subunit mRNAs in adult rat lung by in situ hybridization. *Am J Physiol Lung Cell Mol Physiol* 271: L332–L339, 1996.
174. MAY A, PUOTI A, GAEGGELER HP, HORISBERGER JD, AND ROSSIER BC. Early effect of aldosterone on the rate of synthesis of the epithelial sodium channel alpha subunit in A6 renal cells. *J Am Soc Nephrol* 8: 1813–1822, 1997.
175. MCCLESKEY EW AND GOLD MS. Ion channels of nociception. *Annu Rev Physiol* 61: 835–856, 1999.
176. MCDONALD FJ, YANG B, HRSTKA RF, DRUMMOND HA, TARR DE, MCCRAY PB JR, STOKES JB, WELSH MJ, AND WILLIAMSON RA. Disruption of the beta subunit of the epithelial Na^+ channel in mice: hyperkalemia and neonatal death associated with a pseudohypoaldosteronism phenotype. *Proc Natl Acad Sci USA* 96: 1727–1731, 1999.
177. MCNICHOLAS CM AND CANESSA CM. Diversity of channels generated by different combinations of epithelial sodium channel subunits. *J Gen Physiol* 109: 681–692, 1997.
178. MORAIS-CABRAL JH, ZHOU YF, AND MACKINNON R. Energetic optimization of ion conduction rate by the K^+ selectivity filter. *Nature* 414: 37–42, 2001.
179. MULDERS SM, BICHET DG, RIJSS JP, KAMSTEEG EJ, ARTHUS MF, LONERGAN M, FUJIWARA M, MORGAN K, LEIJENDEKKER R, VAN DER SLUIJS P, VAN OS CH, AND DEEN PM. An aquaporin-2 water channel mutant

which causes autosomal dominant nephrogenic diabetes insipidus is retained in the Golgi complex. *J Clin Invest* 102: 57–66, 1998.
180. Naray-Fejes-Toth A, Canessa C, Cleaveland ES, Aldrich G, and Fejes-Toth G. Sgk is an aldosterone-induced kinase in the renal collecting duct: effects on epithelial Na^+ channels. *J Biol Chem* 274: 16973–16978, 1999.
181. Nielsen S, Chou CL, Marples D, Christensen EI, Kishore BK, and Knepper MA. Vasopressin increases water permeability of kidney collecting duct by inducing translocation of aquaporin-CD water channels to plasma membrane. *Proc Natl Acad Sci USA* 92: 1013–1017, 1995.
182. Nishimoto G, Zelenina M, Li D, Yasui M, Aperia A, Nielsen S, and Nairn AC. Arginine vasopressin stimulates phosphorylation of aquaporin-2 in rat renal tissue. *Am J Physiol Renal Physiol* 276: F254–F259, 1999.
183. Oda Y, Imanzahrai A, Kwong A, Komuves L, Elias PM, Largman C, and Mauro T. Epithelial sodium channels are upregulated during epidermal differentiation. *J Invest Dermatol* 113: 796–801, 1999.
184. Palmer L, Sackin H, and Frindt G. Regulation of Na^+ channels by luminal Na^+ in rat cortical collecting tubule. *J Physiol* 509: 151–162, 1998.
185. Palmer LG. Ion selectivity of the apical membrane Na channel in the toad urinary bladder. *J Membr Biol* 67: 91–98, 1982.
186. Palmer LG. Voltage-dependent block by amiloride and other monovalent cations of apical Na channels in the toad urinary bladder. *J Membr Biol* 80: 153–165, 1984.
187. Palmer LG. Epithelial Na channels: the nature of the conducting pore. *Renal Physiol Biochem* 13: 51–58, 1990.
188. Palmer LG. Commentary: epithelial Na channels. Why all the subunits? *J Gen Physiol* 109: 675–676, 1997.
189. Palmer LG and Andersen OS. Interactions of amiloride and small monovalent cations with the epithelial sodium channel. Inferences about the nature of the channel pore. *Biophys J* 55: 779–787, 1989.
190. Palmer LG and Frindt G. Amiloride-sensitive Na channels from the apical membrane of the rat cortical collecting tubule. *Proc Natl Acad Sci USA* 83: 2727–2770, 1986.
191. Palmer LG and Frindt G. Effects of cell Ca and pH on Na channels from rat cortical collecting tubule. *Am J Physiol Renal Fluid Electrolyte Physiol* 253: F333–F339, 1987.
192. Palmer LG and Frindt G. Conductance and gating of epithelial Na channels from rat cortical collecting tubule. Effects of luminal Na and Li. *J Gen Physiol* 92: 121–138, 1988.
193. Palmer LG and Frindt G. Gating of Na channels in the rat cortical collecting tubule: effects of voltage and membrane stretch. *J Gen Physiol* 107: 35–45, 1996.
194. Park EC and Horvitz HR. Mutations with dominant effects on the behavior and morphology of the nematode *Caenorhabditis elegans*. *Genetics* 113: 821–852, 1986.
195. Pearce D. The role of SGK1 in hormone-regulated sodium transport. *Trends Endocrinol Metab* 12: 341–347, 2001.
196. Perry SJ, Straub VA, Schofield MG, Burke JF, and Benjamin PR. Neuronal expression of an FMRFamide-gated Na^+ channel and its modulation by acid pH. *J Neurosci* 21: 5559–5567, 2001.
197. Poet M, Tauc M, Lingueglia E, Cance P, Poujeol P, Lazdunski M, and Counillon L. Exploration of the pore structure of a peptide-gated Na^+ channel. *EMBO J* 20: 5595–5602, 2001.
198. Pradervand S, Barker PM, Wang Q, Ernst SA, Beermann F, Grubb BR, Burnier M, Schmidt A, Bindels RJ, Gatzy JT, Rossier BC, and Hummler E. Salt restriction induces pseudohypoaldosteronism type 1 in mice expressing low levels of the beta-subunit of the amiloride-sensitive epithelial sodium channel. *Proc Natl Acad Sci USA* 96: 1732–1737, 1999.
199. Pradervand S, Wang Q, Burnier M, Beermann F, Horisberger JD, Hummler E, and Rossier BC. A mouse model for Liddle's syndrome. *J Am Soc Nephrol* 10: 2527–2533, 1999.
200. Price MP, Lewin GR, McIlwrath SL, Cheng C, Xie J, Heppenstall PA, Stucky CL, Mannsfeldt AG, Brennan TJ, Drummond HA, Qiao J, Benson CJ, Tarr DE, Hrstka RF, Yang B, Williamson RA, and Welsh MJ. The mammalian sodium channel BNC1 is required for normal touch sensation. *Nature* 407: 1007–1011, 2000.
201. Price MP, Snyder PM, and Welsh MJ. Cloning and expression of a novel human brain Na^+ channel. *J Biol Chem* 271: 7879–7882, 1996.
202. Rao US, Mehdi A, and Steimle RE. Expression of amiloride-sensitive sodium channel: a strategy for the coexpression of multimeric membrane protein in Sf9 insect cells. *Anal Biochem* 286: 206–213, 2000.
203. Reeh PW and Steen KH. Tissue acidosis in nociception and pain. *Prog Brain Res* 113: 143–151, 1996.
204. Reif MC, Troutman SL, and Schafer JA. Sodium transport by rat cortical collecting tubule. Effects of vasopressin and desoxycorticosterone. *J Clin Invest* 77: 1291–1298, 1986.
205. Renard S, Lingueglia E, Voilley N, Lazdunski M, and Barbry P. Biochemical analysis of the membrane topology of the amiloride-sensitive Na^+ channel. *J Biol Chem* 269: 12981–12986, 1994.
206. Robert-Nicoud M, Flahaut M, Elalouf JM, Nicod M, Salinas M, Bens M, Doucet A, Wincker P, Artiguenave F, Horisberger JD, Vandewalle A, Rossier BC, and Firsov D. Transcriptome of a mouse kidney cortical collecting duct cell line: effects of aldosterone and vasopressin. *Proc Natl Acad Sci USA* 98: 2712–2716, 2001.
207. Robinson DH, Bubien JK, Smith PR, and Benos DJ. Epithelial sodium conductance in rabbit preimplantation trophectodermal cells. *Dev Biol* 147: 313–321, 1991.
208. Rossier BC, Canessa CM, Schild L, and Horisberger JD. Epithelial sodium channels. *Curr Opin Nephrol Hypertens* 3: 487–496, 1994.
209. Rossier BC, Pradervand S, Schild L, and Hummler E. Epithelial sodium channel and the control of sodium balance: interaction between genetic and environmental factors. *Annu Rev Physiol* 64: 877–897, 2002.
210. Roudier-Pujol C, Rochat A, Escoubet B, Eugene E, Barrandon Y, and Bonvalet JPFN. Differential expression of epithelial sodium channel subunit mRNAs in rat skin. *J Cell Sci* 109: 379–385, 1996.
211. Ruben P, Johnson JW, and Thompson S. Analysis of FMRF-amide effects on *Aplysia* bursting neurons. *J Neurosci* 6: 252–259, 1986.
212. Sakai H, Lingueglia E, Champigny G, Mattei MG, and Lazdunski M. Cloning and functional expression of a novel degenerin-like Na^+ channel gene in mammals. *J Physiol* 519: 323–333, 1999.
213. Saxena A, Hanukoglu I, Strautnieks SS, Thompson RJ, Gardiner RM, and Hanukoglu A. Gene structure of the human amiloride-sensitive epithelial sodium channel beta subunit. *Biochem Biophys Res Commun* 252: 208–213, 1998.
214. Sayegh R, Auerbach SD, Li X, Loftus RW, Husted RF, Stokes JB, and Thomas CP. Glucocorticoid induction of epithelial sodium channel expression in lung and renal epithelia occurs via transactivation of a hormone response element in the 5′-flanking region of the human epithelial sodium channel alpha subunit gene. *J Biol Chem* 274: 12431–12437, 1999.
215. Schaedel C, Marthinsen L, Kristoffersson AC, Kornfalt R, Nilsson KO, Orlenius B, and Holmberg L. Lung symptoms in pseudohypoaldosteronism type 1 are associated with deficiency of the alpha-subunit of the epithelial sodium channel. *J Pediatr* 135: 739–745, 1999.
216. Schaefer L, Sakai H, Mattei MG, Lazdunski M, and Lingueglia E. Molecular cloning, functional expression and chromosomal localization of an amiloride-sensitive Na^+ channel from human small intestine. *FEBS Lett* 471: 205–210, 2000.
217. Schafer JA and Hawk CT. Regulation of Na^+ channels in the cortical collecting duct by AVP and mineralocorticoids. *Kidney Int* 41: 255–268, 1992.
218. Schild L, Canessa CM, Shimkets RA, Gautschi I, Lifton RP, and Rossier BC. A mutation in the epithelial sodium channel causing Liddle disease increases channel activity in the *Xenopus laevis* oocyte expression system. *Proc Natl Acad Sci USA* 92: 5699–5703, 1995.
219. Schild L, Lu Y, Gautschi I, Schneeberger E, Lifton RP, and Rossier BC. Identification of a PY motif in the epithelial Na channel subunits as a target sequence for mutations causing channel activation found in Liddle syndrome. *EMBO J* 15: 2381–2387, 1996.
220. Schild L, Schneeberger E, Gautschi I, and Firsov D. Identification of amino acid residues in the α, β, γ subunits of the epithelial sodium channel (ENaC) involved in amiloride block and ion permeation. *J Gen Physiol* 109: 15–26, 1997.
221. Schwartz GJ and Burg MB. Mineralocorticoid effects on cation transport by cortical collecting tubules in vitro. *Am J Physiol Renal Fluid Electrolyte Physiol* 235: F576–F585, 1978.
222. Sheng S, McNulty KA, Harvey JM, and Kleyman TR. Second trans-

membrane domains of ENaC subunits contribute to ion permeation and selectivity. *J Biol Chem* 276: 44091–44098, 2001.
223. SHENG SH, LI JQ, MCNULTY KA, AVERY D, AND KLEYMAN TR. Characterization of the selectivity filter of the epithelial sodium channel. *J Biol Chem* 275: 8572–8581, 2000.
224. SHI H, ASHER C, CHIGAEV A, YUNG Y, REUVENY E, SEGER R, AND GARTY H. Interactions of beta and gamma ENaC with Nedd4 can be facilitated by an EKR-mediated phosphorylation. *J Biol Chem* 277: 13539–13547, 2002.
225. SHIMKETS RA, LIFTON R, AND CANESSA CM. In vivo phosphorylation of the epithelial sodium channel. *Proc Natl Acad Sci USA* 95: 3301–3305, 1998.
226. SHIMKETS RA, LIFTON RP, AND CANESSA CM. The activity of the epithelial sodium channel is regulated by clathrin-mediated endocytosis. *J Biol Chem* 272: 25537–25541, 1997.
227. SILVER RB, FRINDT G, WINDHAGER EE, AND PALMER LG. Feedback regulation of Na channels in rat CCT. I. Effects of inhibition of Na pump. 264: F557–F564, 1993.
228. SNYDER PM, BUCHER DB, AND OLSON DR. Gating induces a conformational change in the outer vestibule of ENaC. *J Gen Physiol* 116: 781–790, 2000.
229. SNYDER PM, CHENG C, PRINCE LS, ROGERS JC, AND WELSH MJ. Electrophysiological and biochemical evidence that DEG/ENaC cation channels are composed of nine subunits. *J Biol Chem* 273: 681–684, 1998.
230. SNYDER PM, MCDONALD FJ, STOKES JB, AND WELSH MJ. Membrane topology of the amiloride-sensitive epithelial sodium channel. *J Biol Chem* 269: 24379–24383, 1994.
231. SNYDER PM, OLSON DR, AND BUCHER DB. A pore segment in DEG/ENaC Na^+ channels. *J Biol Chem* 274: 28484–28490, 1999.
232. SNYDER PM, PRICE MP, MCDONALD FJ, ADAMS CM, VOLK KA, ZEIHER BG, STOKES JB, AND WELSH MJ. Mechanism by which Liddle's syndrome mutations increase activity of a human epithelial Na^+ channel. *Cell* 83: 969–978, 1995.
233. SOMJEN GG. Acidification of interstitial fluid in hippocampal formation caused by seizures and by spreading depression. *Brain Res* 311: 186–188, 1984.
234. STARKUS JG, KUSCHEL L, RAYNER MD, AND HEINEMANN SH. Ion conduction through C-type inactivated Shaker channels. *J Gen Physiol* 110: 539–550, 1997.
235. STAUB O, DHO S, HENRY P, CORREA J, ISHIKAWA T, MCGLADE J, AND ROTIN D. WW domains of Nedd4 bind to the proline-rich PY motifs in the epithelial Na^+ channel deleted in Liddle's syndrome. *EMBO J* 15: 2371–2380, 1996.
236. STAUB O, GAUTSCHI I, ISHIKAWA T, BREITSCHOPF K, CIECHANOVER A, SCHILD L, AND ROTIN D. Regulation of stability and function of the epithelial Na^+ channel (ENaC) by ubiquitination. *EMBO J* 16: 6325–6336, 1997.
237. STOKES JB AND SIGMUND RD. Regulation of rENaC mRNA by dietary NaCl and steroids: organ, tissue, and steroid heterogeneity. *Am J Physiol Cell Physiol* 43: C1699–C1707, 1998.
238. STRAUTNIEKS SS, THOMPSON RJ, GARDINER RM, AND CHUNG E. A novel splice-site mutation in the gamma subunit of the epithelial sodium channel gene in three pseudohypoaldosteronism type 1 families. *Nature Genet* 13: 248–250, 1996.
239. SURPRENANT A, RASSENDREN F, KAWASHIMA E, NORTH RA, AND BUELL G. The cytolytic P2Z receptor for extracellular ATP identified as a P2X receptor (P2X7). *Science* 272: 735–738, 1996.
240. SUTHERLAND SP, BENSON CJ, ADELMAN JP, AND MCCLESKEY EW. Acid-sensing ion channel 3 matches the acid-gated current in cardiac ischemia-sensing neurons. *Proc Natl Acad Sci USA* 98: 711–716, 2001.
241. TAKE-UCHI M, KAWAKAMI M, ISHIHARA T, AMANO T, KONDO K, AND KATSURA I. An ion channel of the degenerin/epithelial sodium channel superfamily controls the defecation rhythm in *Caenorhabditis elegans*. *Proc Natl Acad Sci USA* 95: 11775–11780, 1998.
242. TALBOT CL, BOSWORTH DG, BRILEY EL, FENSTERMACHER DA, BOUCHER RC, GABRIEL SE, AND BARKER PM. Quantitation and localization of ENaC subunit expression in fetal, newborn, and adult mouse lung. *Am J Respir Cell Mol Biol* 20: 398–406, 1999.
243. TAVERNARAKIS N AND DRISCOLL M. Molecular modeling of mechanotransduction in the nematode *Caenorhabditis elegans*. *Annu Rev Physiol* 59: 659–689, 1997.
244. TAVERNARAKIS N AND DRISCOLL M. *Caenorhabditis elegans* degenerins and vertebrate ENaC ion channels contain an extracellular domain related to venom neurotoxins. *J Neurogenet* 13: 257–264, 2000.
245. TAVERNARAKIS N, SHREFFLER W, WANG SL, AND DRISCOLL M. Unc-8, a deg/enac family member, encodes a subunit of a candidate mechanically gated channel that modulates *C. elegans* locomotion. *Neuron* 18: 107–119, 1997.
246. THE *C. ELEGANS* SEQUENCING CONSORTIUM. Genome sequence of the nematode *C. elegans*: a platform for investigating biology. *Science* 282: 2012–2018, 1998.
247. THOMAS CP, AUERBACH S, STOKES JB, AND VOLK KA. 5′ Heterogeneity in epithelial sodium channel alpha-subunit mRNA leads to distinct NH_2-terminal variant proteins. *Am J Physiol Cell Physiol* 274: C1312–C1323, 1998.
248. THOMAS CP, AUERBACH SD, ZHANG C, AND STOKES JB. The structure of the rat amiloride-sensitive epithelial sodium channel gamma subunit gene and functional analysis of its promoter. *Gene* 228: 111–122, 1999.
249. THOMAS CP, DOGGETT NA, FISHER R, AND STOKES JB. Genomic organization and the 5′ flanking region of the gamma subunit of the human amiloride-sensitive epithelial sodium channel. *J Biol Chem* 271: 26062–26066, 1996.
250. UGAWA S, MINAMI Y, GUO W, SAISHIN Y, TAKATSUJI K, YAMAMOTO T, TOHYAMA M, AND SHIMADA S. Receptor that leaves a sour taste in the mouth. *Nature* 395: 555–556, 1998.
251. UGAWA S, UEDA T, MINAMI Y, HORIMOTO M, AND SHIMADA S. A single amino acid substitution in MDEG2 specifically alters desensitization of the proton-activated cation current. *Neuroreport* 12: 2141–2145, 2001.
252. UGAWA S, UEDA T, TAKAHASHI E, HIRABAYASHI Y, YONEDA T, KOMAI S, AND SHIMADA S. Cloning and functional expression of ASIC-beta 2, a splice variant of ASIC-beta. *Neuroreport* 12: 2865–2869, 2001.
253. URBANICS R, LENIGER-FOLLERT E, AND LUBBERS DW. Time course of changes of extracellular H^+ and K^+ activities during and after direct electrical stimulation of the brain cortex. *Pflügers Arch* 378: 47–53, 1978.
254. VALLET V, CHRAIBI A, GAEGGELER HP, HORISBERGER JD, AND ROSSIER BC. An epithelial serine protease activates the amiloride-sensitive sodium channel. *Nature* 389: 607–610, 1997.
255. VARMING T. Proton-gated ion channels in cultured mouse cortical neurons. *Neuropharmacology* 38: 1875–1881, 1999.
256. VENTER JC, ADAMS MD, MYERS EW, LI PW, MURAL RJ, SUTTON GG, SMITH HO, YANDELL M, EVANS CA ET AL. The sequence of the human genome. *Science* 291: 1304–1351, 2001.
257. VERREY F, HUMMLER E, SCHILD L, AND ROSSIER BC. Control of Na^+ transport by aldosterone. In: *The Kidney. Physiology and Pathophysiology* (3rd ed.), edited by Seldin DW and Giebisch G. Philadelphia, PA: Lippincott Williams & Wilkins, 2000, p. 1441–1472.
258. VIRGINIO C, MACKENZIE A, RASSENDREN FA, NORTH RA, AND SURPRENANT A. Pore dilation of neuronal P2X receptor channels. *Nature Neurosci* 2: 315–321, 1999.
259. VOILLEY N, DEWEILLE J, MAMET J, AND LAZDUNSKI M. Nonsteroid anti-inflammatory drugs inhibit both the activity and the inflammation-induced expression of acid-sensing ion channels in nociceptors. *J Neurosci* 21: 8026–8033, 2001.
260. VOLK KA, SIGMUND RD, SNYDER PM, MCDONALD J, WELSH MJ, AND STOKES JB. rENaC is the predominant Na^+ channel in the apical membrane of the rat renal inner medullary collecting duct. *J Clin Invest* 96: 2748–2757, 1995.
261. VOÛTE CL, DIRIX R, NIELSEN R, AND USSING HH. The effect of aldosterone on the isolated frog skin epithelium (*R. temporaria*): a morphological study. *Exp Cell Res* 57: 448, 1969.
262. VUAGNIAUX G, VALLET V, JAEGER NF, PFISTER C, BENS M, FARMAN N, COURTOIS-COUTRY N, VANDEWALLE A, ROSSIER BC, AND HUMMLER E. Activation of the amiloride-sensitive epithelial sodium channel by the serine protease mCAP1 expressed in a mouse cortical collecting duct cell line. *J Am Soc Nephrol* 11: 828–834, 2000.
263. WALDMANN R, BASSILANA F, DEWEILLE J, CHAMPIGNY G, HEURTEAUX C, AND LAZDUNSKI M. Molecular cloning of a non-inactivating proton-gated Na^+ channel specific for sensory neurons. *J Biol Chem* 272: 20975–20978, 1997.

264. WALDMANN R, CHAMPIGNY G, BASSILANA F, HEURTEAUX C, AND LAZDUNSKI M. A proton-gated cation channel involved in acid-sensing. *Nature* 386: 173–177, 1997.
265. WALDMANN R, CHAMPIGNY G, BASSILANA F, VOILLEY N, AND LAZDUNSKI M. Molecular cloning and functional expression of a novel amiloride-sensitive Na^+ channel. *J Biol Chem* 270: 27411–27414, 1995.
266. WALDMANN R, CHAMPIGNY G, VOILLEY N, LAURITZEN I, AND LAZDUNSKI M. The mammalian degenerin MDEG, an amiloride-sensitive cation channel activated by mutations causing neurodegeneration in *Caenorhabditis elegans*. *J Biol Chem* 271: 10433–10436, 1996.
267. WALDMANN R AND LAZDUNSKI M. H^+-gated cation channels: neuronal acid sensors in the NaC/DEG family of ion channels. *Curr Opin Neurobiol* 8: 418–424, 1998.
268. WALDMANN R, VOILLEY N, MATT MG, AND LAZDUNSKI M. The human degenerin MDEG, an amiloride-sensitive neuronal cation channel, is localized on chromosome 17q11.2–17q12 close to the microsatellite D17S798. *Genomics* 37: 269–270, 1996.
269. WOOD JN. Pathobiology of visceral pain: molecular mechanisms and therapeutic implications. II. Genetic approaches to pain therapy. *Am J Physiol Gastrointest Liver Physiol* 278: G507–G512, 2000.
270. XIONG ZQ AND STRINGER JL. Extracellular pH responses in CA1 and the dentate gyrus during electrical stimulation, seizure discharges, and spreading depression. *J Neurophysiol* 83: 3519–3524, 2000.
271. ZEISKE W AND LINDEMANN B. Chemical stimulation of Na current through the outer surface of frog skin epithelium. *Biochim Biophys Acta* 352: 323–326, 1974.
272. ZHAINAZAROV AB AND COTTRELL GA. Single-channel currents of a peptide-gated sodium channel expressed in *Xenopus* oocytes. *J Physiol (Lond)* 513: 19–31, 1998.
273. ZHOU YF, MORAIS-CABRAL JH, KAUFMAN A, AND MACKINNON R. Chemistry of ion coordination and hydration revealed by a K^+ channel-Fab complex at 2.0 angstrom resolution. *Nature* 414: 43–48, 2001.
274. ZUCKERMAN JB, CHEN X, JACOBS JD, HU B, KLEYMAN TR, AND SMITH PR. Association of the epithelial sodium channel with Apx and alpha-spectrin in A6 renal epithelial cells. *J Biol Chem* 274: 23286–23295, 1999.